3

Steady drag forces

3.1 Introduction

ACVs and SESs create drag forces as they move over the water surface. The most important drag components are those due to friction with immersed components such as sidewalls, skirt, propellers, rudders and other appendages; and wave-making drag from the moving cushion pressure field and sidewalls. In addition, momentum drag due to acceleration of the air used for the supporting air cushion, and aerodynamic profile drag of the ACV or SES become important components at higher speeds.

In this chapter we will outline the theory behind these drag components and describe methods for their estimation.

3.2 Classification of drag components

The method of calculating drag forces on an ACV or SES is similar to that for predicting the drag of a planing hull or a sea plane before take-off. ACVs and SES also generate spray drag, skirt friction drag and skirt inertia drag in addition to the water drag components associated with a normal ship. For this reason drag calculations are more complicated than for other marine craft.

Based upon calculation methods for predicting the drag of a planing hull, the principal author and colleagues at MARIC have developed a methodology for predicting the drag for ACV/SES which may be summarized as follows:

- First of all we obtain the total drag from model tests in a towing tank and some other main components of drag by means of reliable and practical methods, e.g. according to the Reynolds analogue theory to obtain the test results in wind tunnels for predicting air profile drag.
- Then the residual drag of models can be determined by deducting the main components of drag which can be calculated individually, from the total drag of the model measurements.

According to Froude's analogue theory we can define the residual drag of full-scale ships from that of models; consequently the total drag for a full-scale ship can be

obtained by adding the residual drag of the ship to the main components of ship drag which can be determined by calculations.

In general, the total drag of craft can be written as follows:

$$R_{acv} = R_w + R_a + R_m + R_{sk} + R_{a''}$$

or

$$R_{ses} = R_w + R_a + R_m + R_{sk} + R_{swf} + R_{ap} + R_{mw} + R_{a''}$$

where R_{acv} is the ACV total drag; R_{ses} the SES total drag; R_w the wave-making drag due to the air cushion; R_a the aerodynamic profile drag; R_m the aerodynamic momentum drag; R_{sk} the skirt drag for ACVs and bow/stern seal drag for SESs; R_{swf} the friction drag of sidewalls; R_{ap} the underwater appendage drag (e.g. rudders, air ingestion fences, propeller brackets); R_{mw} the hydrodynamic momentum drag due to the cooling water of engines and $R_{a''}$ the drag due to the differential air momentum leakage from bow and stern skirts.

Fig. 3.1 shows the various components of drag of the SES-100A built in the USA. The principal dimensions and parameters of the SES-100A are $L/B = 2.16$, $p_c/L_c = 19.5$ kgf/m, $v_{max} = 76$ knots.

The following sections of this chapter outline the methodology for determination of each drag component listed above.

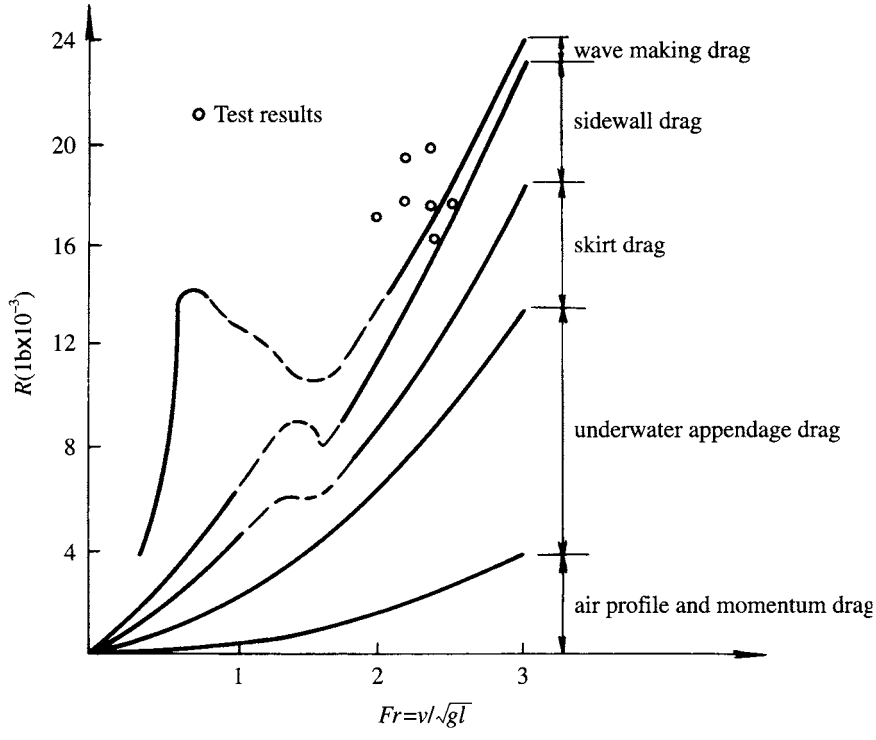

Fig. 3.1 SES-100A drag as a function of Froude number.

3.3 Air cushion wave-making drag (R_w)

Wave-making drag generated by a pressure distribution is a classical theme of hydrodynamics, since a ship's hull is generally represented by a surface consisting of a varying potential function which applies positive pressure in the forebody and suction pressure around the stern [8,17].

The equivalent problem for a hovercraft was addressed by Newman and Poole [18], who derived a calculation method for predicting the wave-making drag. They simplified the air cushion to an equivalent rectangular surface with a uniform pressure distribution and calculated the wave-making drag as

$$R_w = C_w \left[\frac{p_c^2 . B_c}{(\rho_w . g)}\right] \tag{3.1}$$

where

$$C_w = f\,(F_{r_1} \text{ and } l_c/B_c)$$

and R_w is the wave-making drag due to air cushion, (N), p_c the cushion pressure (N/m^2), B_c the cushion beam, (m), l_c the cushion length (m), ρ_w the water mass density (0.10177 − 0.1045) (N s^2/m^4), g the gravitational acceleration (9.8066)(m/s^2) and C_w the wave-making drag coefficient due to the air cushion travelling on a waterway with infinite depth, as shown in Fig. 3.2.

Figure 3.2 shows that as cushion length is increased, so the primary hump at F_r approx. 0.56 reduces. Craft with l_c/B_c in the range 2–4 have a significantly higher drag peak at F_r approx. 0.33, so thrust margin at this speed should also be checked during design. Figure 3.3 shows the variation of C_w against l_c/B_c for various F_r, interpreted from Fig. 3.2. It can be seen that below l_c/B_c of about 6, the primary drag hump at F_r 0.56 begins to build up. Figure 3.4 shows plots of C_w vs F_r for selected l_c/B_c, taken from Fig. 3.3.

It is important to note here that wave-making drag is proportional to p_c^2 and the cushion width. Craft drag can therefore be significantly reduced by increasing craft length. This was used successfully by BHC in stretching the SR.N6 craft in the UK, and the US Navy SES-100 to SES-200.

In fact, the wave-making drag can be defined as

$$\frac{R_w}{p_c S_c} = \frac{R_w}{W} = \sin \alpha' \tag{3.2}$$

where $\alpha - \alpha'$ is the average slope of the wave generated by a moving air cushion. This is most suitable for a cushion moving at high F_r, generating a wave, rather longer than cushion length.

Meanwhile, equation (3.1) can also be written as

$$\frac{R_w}{W} = C_w \left[\frac{p_c^2 B_c}{\rho_w g W}\right]$$

$$= C_w \cdot \frac{1}{\rho_w g} \cdot \frac{p_c}{l_c} \tag{3.3}$$

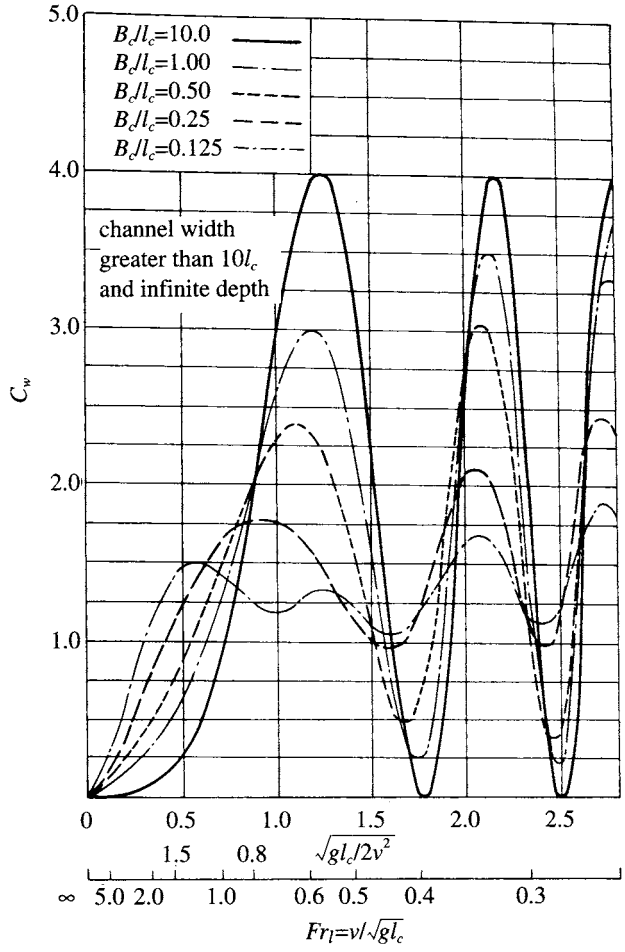

Fig. 3.2 C_w plotted against F_{rl} for constant L_c/B_c.

or

$$\frac{R_w}{W} = f\,(F_{r_l}, l_c/B_{c,}, p_c/l_c)$$

where p_c/l_c is the pressure/length ratio of hovercraft.

As mentioned above, the wave-making drag is a function of cushion length to beam ratio, pressure to length ratio and Froude number. The cushion length/beam ratio therefore plays a significant role in the craft performance.

Reference 19 also offered another similar formula for estimating the wave-making drag:

$$R_w = C_w(4\,p_c\,W)/(\rho_w\,g\,l_c) \tag{3.4}$$

where l_c is the equivalent cushion length, i.e. $l_c = S_c/B_c$, S_c the cushion area, B_c the cushion beam and C_w the wave-making drag coefficient as shown in Fig. 3.4.

It should be noted that it is best to use the formula above together with formulae

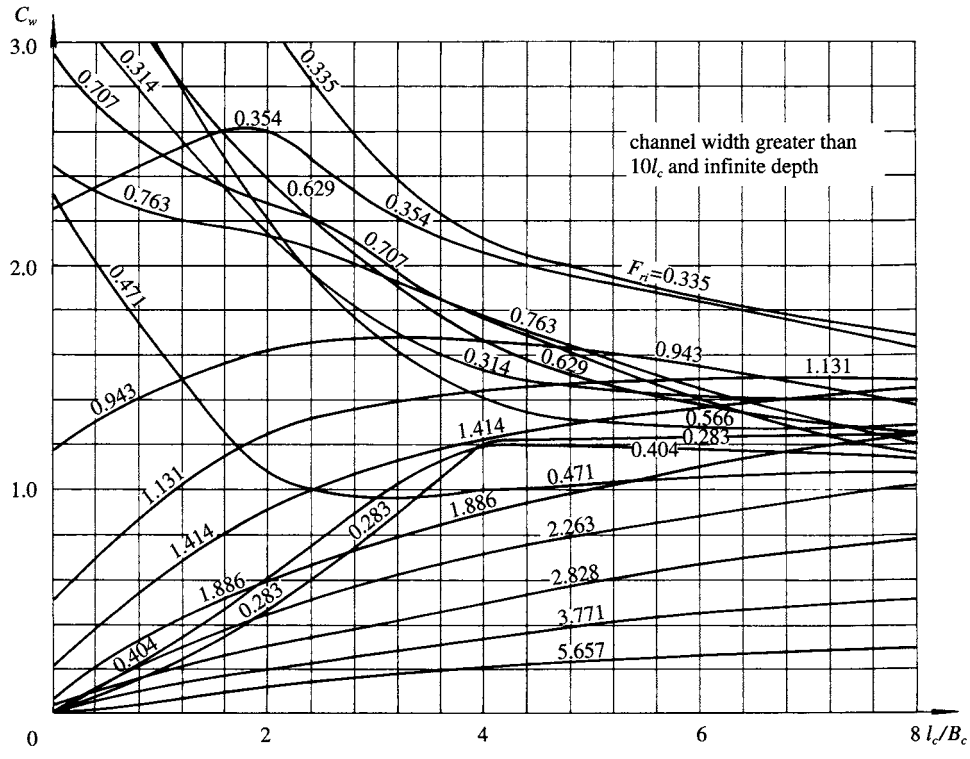

Fig. 3.3 Cushion wave-making drag coefficient for a rectangular air cushion over calm water against L_c/B_c.

predicting the other components of drag also developed by the same authors, e.g. when one uses the equation (3.4) for estimating the wave-making drag, it is better to use this together with the other formulae offered by ref. 19 for estimating the seal drag, sidewall water friction and the residual drag of sidewalls, otherwise the user may find inconsistencies in calculation of the total resistance of the ACV.

Owing to the easy application and accuracy of Newman's method, MARIC often uses Newman and Poole's data for estimating the wave-making resistance of craft. It is evident from this work that the bow wave strongly interacts with the stern wave. The lower the cushion beam ratio, the stronger the disturbance between the two components. This causes a series of peaks and troughs on the resistance curve. With respect to water with infinite depth, the last peak appears at $Fr = 1/\sqrt{\pi} \cong 0.56$.

The theory mentioned above was validated by the experimental results carried out by Everest and Hogben [20]. The theoretical prediction agreed quite well with experimental results except at low speed. In this latter case, only two pairs of troughs and peaks appeared in the test results rather than that in the calculation results. This can be interpreted as follows:

- Hogben proposed that the wave steepness (h/λ) at lower Fr predicted by linear theoretical calculation exceeded the theoretical limit value of 1/7 between the troughs and peaks, so that the surface geometry would be unstable, similar to a

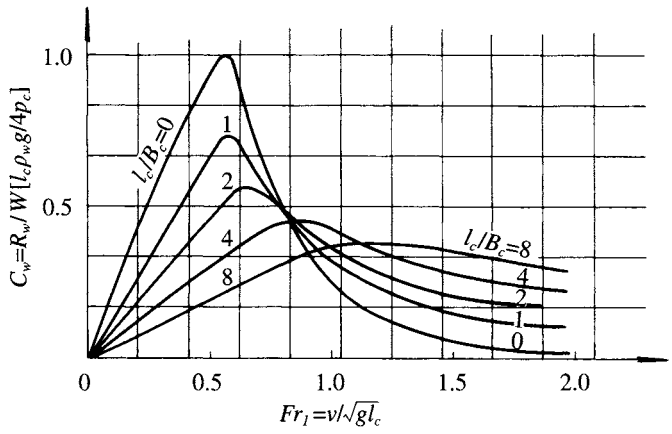

Fig. 3.4 C_w plotted against F_{rl} for constant L_c/B_c.

breaking wave. The linear assumptions in wave-making theory have to be replaced by nonlinear wave-making theory at these *Fr*.

- Doctors [21] considered the predicted sharp peaks and troughs at low *Fr* are caused by assuming a uniform pressure distribution, which implies a step pressure change at the bow and stern, which clearly is not reflected in reality. The sharp peaks and troughs will disappear and the theoretical prediction will agree quite well with test results, when one assumes the uniform distribution of pressure inside the cushion is combined with a smooth pressure transient at the bow and stern (or the whole periphery for an ACV) with hyperbolic decay to ambient.

Since then, Bolshakov has calculated the wave-making drag of an air cushion with uniform distribution of cushion pressure with a round bow and square stern in horizontal plane (similar to an SR.N5 or SR.N6). Tatinclaux [22] has extended these data by calculating the velocity potential and wave-making of air cushions with uniform cushion pressure distribution and various plan shapes such as rectangle, circle and semicircles. Because the velocity potential used is linear, the potential due to the combined plan shapes of an air cushion can be obtained by the superposition of velocity potentials due to the separate area components, so as to obtain the corresponding total wave-making drag.

Comparing the coefficients for wave-making drag of air cushions of various plan shapes, a rectangular air cushion is found to have the minimum coefficient, particularly near hump speed. The rectangular air cushion will gain more advantage if the drag–lift ratio R_w/W is also considered. This can be demonstrated as follows; first, define a shape factor for the cushion, which is the envelope rectangle, divided by the actual area, by which we have

$$\varphi_s = (l_c\, B_c/S_c)^2$$

also define the non-dimensional cushion pressure/length ratio:

$$\bar{p}_c = \{W/(l_c\, B_c)\}/(\rho_w\, g\, l_c)$$

then

$$R_w/W = C_w \varphi_s \bar{p}_c' \tag{3.5}$$

where R_w/W is the wave-making drag–lift ratio, W the weight of craft and C_w the wave-making drag coefficient.

From this equation we can see that for constant cushion length l_c, cushion beam B_c and craft weight W, the non-dimensional cushion pressure–length ratio $\bar{p}_c$, will stay constant, but φ_s will change with respect to different shape of cushion plan.

For a rectangular air cushion, $\varphi_s = 1$ and will be the minimum, meanwhile C_w will be minimum when the cushion plan is rectangular; therefore an air cushion with rectangular shape will gain more advantage not only on the ratio between wave-making drag and craft weight but also on take-off ability through hump speed.

Selection of the plan shape for an ACV should consider take-off ability, together with seaworthiness and general arrangement of craft, as well as the configuration and fabrication of skirts, etc., not just for minimum drag.

The study mentioned above was based upon the assumption of uniform distribution of air pressure within the cushion and with a discontinuous sudden change of pressure at the cushion edges. The sudden change of pressure distribution can only appear at the sidewalls of an SES, and cannot exist on an ACV with flexible skirts. Therefore this method will make a calculation error for an ACV.

Doctors [21] and Tatinclaux [22] each made studies of the pressure distribution with various rules to overcome this problem. Doctors assumed that the pressure distribution formed a hyperbolic tangent, while Tatinclaux assumed a linear distribution. The calculation results demonstrated that both methods agreed quite well with the calculation results by Newman's method at post-hump speed and did not produce the sharp peaks and troughs in the resistance curve at pre-hump speed (Fig. 3.5).

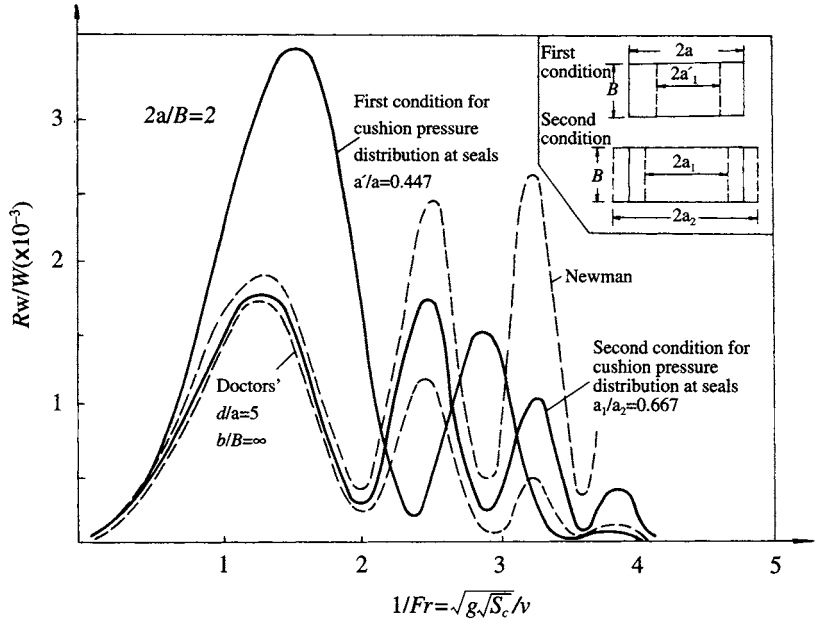

Fig. 3.5 Comparison of wave-making drag between the test results and calculation by various formulae.

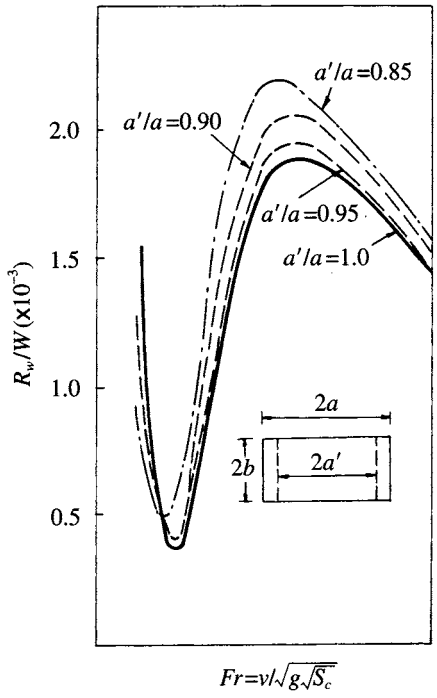

Fig. 3.6 Cushion wave-making drag ratio as a function of equivalent Froude Number. [22]

In addition, Tatinclaux calculated two further pressure distribution combinations, i.e. linear distribution at bow/stern and sudden change at two sides (similar to an SES), as well as distribution at two sides and sudden change at bow/stern (Figs 3.6 and 3.7). It is shown that the first condition influenced the wave-making drag dramatically, but the latter did not. For this reason it is clear that wave-making is mainly generated from the bow and stern (this is similar in principle to the bow and stern wave patterns generated by a normal ship's hull).

With respect to shallow water drag, theoretical calculation demonstrated that wave-making drag in shallow water would be larger than that in water with infinite depth, particularly at hump speed. As water depth reduces, so the drag increases so as to increase the drag hump. When the effect of the water depth on the practical limit for the height of generated waves is taken into account, this limits the maximum wave drag, which is the reason operators can use shallow water to go through hump speed on a marginal craft.

If the progression through craft hump speed was not steady, but accelerating, Tatinclaux showed that the wave-making drag peaks caused by an air cushion with the hyperbolic tangent pressure distribution at the bow/stern running over both deep and shallow water at constant accelerated motion were flattened by the acceleration.

This effect will be strengthened while craft are travelling over shallow water rather than deep water (Figs 3.8 and 3.9). These figures show that the craft peak resistance will decrease in shallow water by accelerated motion, in a similar manner to that on deep water at approximately $Fr = 0.5$. This is another reason why an ACV or SES, particularly with flexible skirts, can pass through the hump speed over shallow water

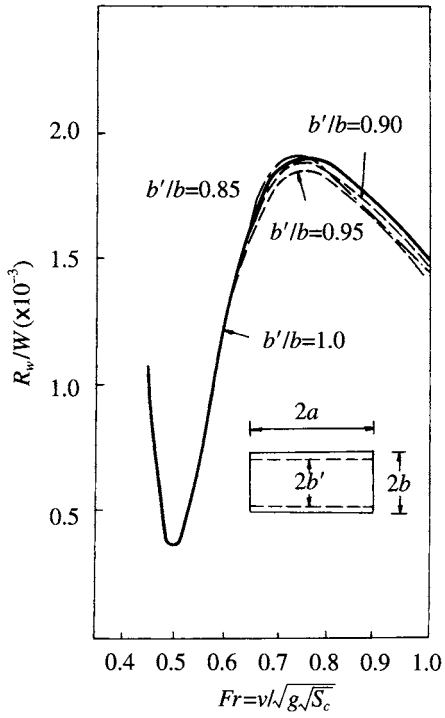

Fig. 3.7 Cushion wave-making drag ratio as a function of equivalent Froude Number. [22]

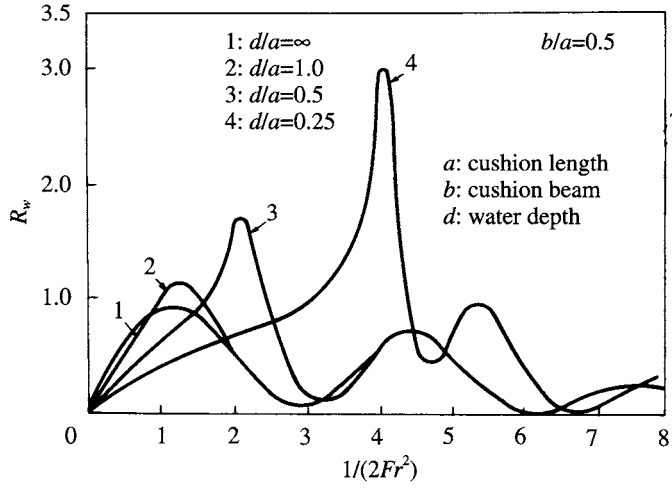

Fig. 3.8 Influence of water depth on cushion wave-making drag.

without special difficulty. Figure 3.10 shows the trial results of a full-scale craft SES–100B. It was found that the drag decreased as the craft accelerated. The drag over both shallow and deep water is presented in Fig. 3.11.

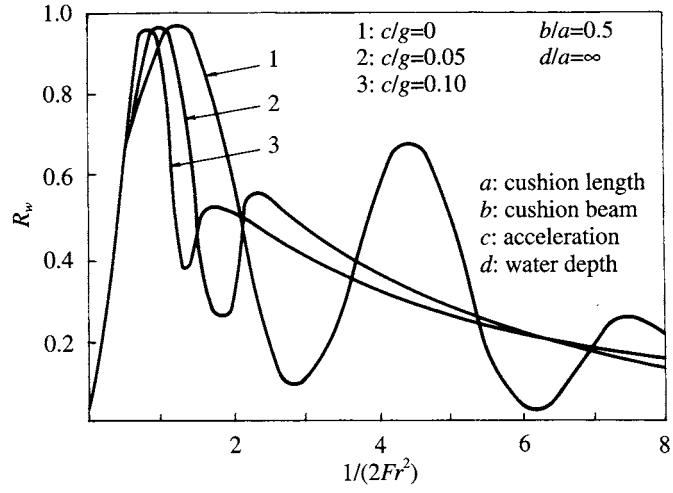

Fig. 3.9 Variation of cushion wave-making drag on accelerating craft. [21]

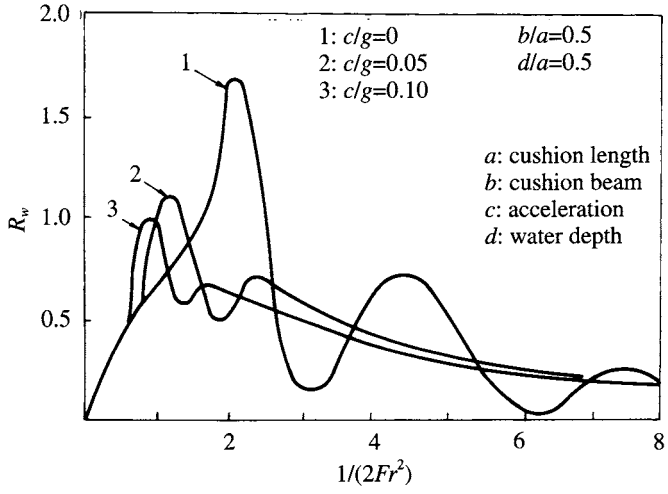

Fig. 3.10 Variation of cushion wave making drag on accelerating craft. [21]

The principal research work into wave-making drag due to an air cushion travelling in yaw was carried out by Tatinclaux, who showed that peak drag of a craft in yaw increased dramatically. MARIC also has practical experience that a craft travelling in yaw on water is very difficult to pass through hump speed, particularly for an amphibious ACV. An ACV travelling in yaw in a beam wind condition will probably have difficulty in passing through the hump speed as well as increasing handling difficulties.

Pilots with such problems in open water will usually make a track across or down wind to accelerate through the hump and then return to the intended course. In more restricted conditions, a downwind track to a more sheltered area where the craft can be turned around over the hump may be needed.

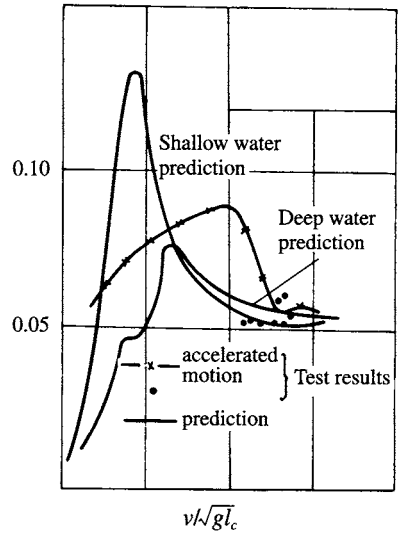

Fig. 3.11 Variation of craft drag/weight ratio on accelerating craft over shallow water.

Figure 3.12 shows the wave-making drag at various F_r, yawing angle, and cushion length–beam ratios. It may be noted that the wave-making drag when yawed is

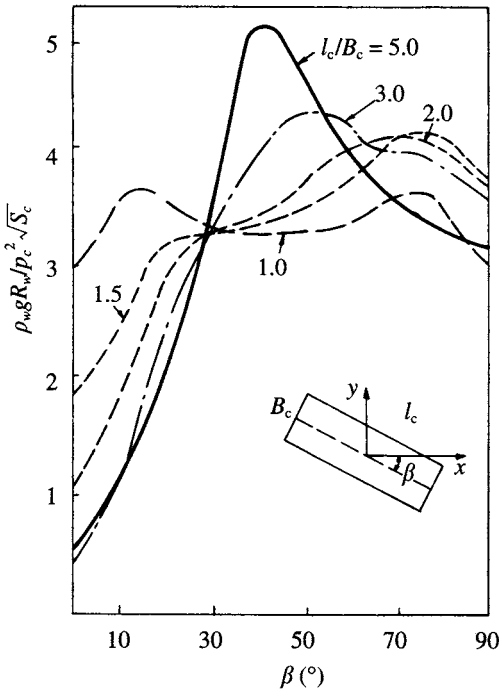

Fig. 3.12(a) Wave-making drag coefficient for yawed craft, $F_r = 0.6$.

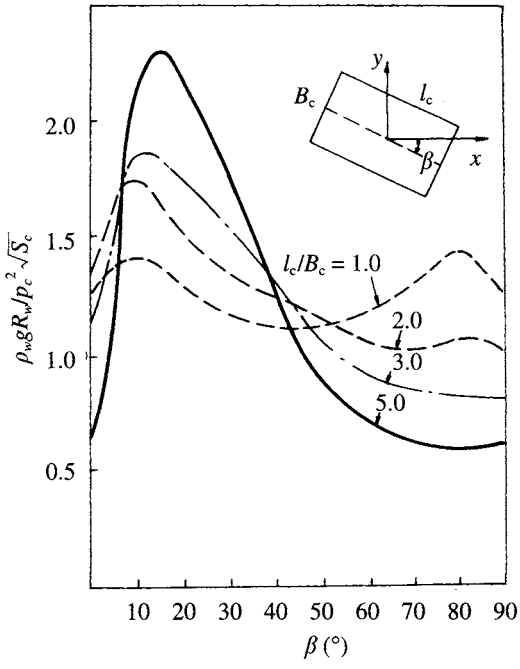

Fig. 3.12(b) Wave-making drag coefficient for yawed craft, $F_r = 1.0$.

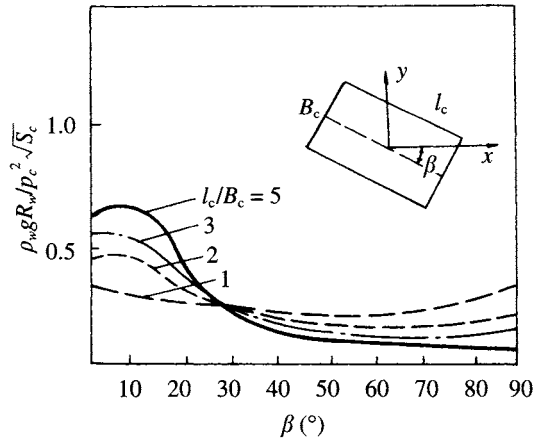

Fig. 3.12(c) Wave-making drag coefficient of yawed craft, $F_r = 2.0$.

several times greater than that on a straight course (if one takes the skirt drag due to the scooping water of the craft in yaw into account, the added drag will increase further).

3.4 Aerodynamic profile drag

The aerodynamic profile drag can be written as

$$R_a = C_a \frac{\rho_a}{2} \cdot S_a v^2 \tag{3.6}$$

where R_a is the aerodynamic profile drag (N), C_a the coefficient for the aerodynamic profile drag and S_a the frontal projecting area of the hull above the water (m^2). C_a is highly sensitive to the aerodynamic profile of the craft's hull, inclusive of the inflated skirt. Its value is generally obtained from wind tunnel tests for detailed design. Table 3.1 gives a selection of C_a data for various models and craft based on wind tunnel data. It can be seen that C_a for an ACV (particularly for passenger craft) is in general small. C_a can be estimated based on the geometry of a new craft, using data such as presented by Hoerner [23] and comparison with known data such as that in Table 3.1.

ACV aerodynamic drag is generally a significant proportion of total drag because of high design craft speed and the low water drag. For example, the aerodynamic drag of ACV 711-A built in China is 30% of the total drag of this craft at a speed at 85 km/h. Therefore it is very important to design an ACV craft superstructure with care.

In general, the C_a can be taken as 0.4–0.6 for an ACV, with extreme values of 0.3 for fine lines and 0.75 for poor lines. For example, C_a for US *Voyageur* and JEFF(B) is 0.75 due to their open well deck for accommodating tanks or large loads. C_a is typically 0.5–0.7 for SES. In the final analysis, it is best to use test results from a wind tunnel if possible, to determine this fraction of the total drag force accurately.

Table 3.1 The aerodynamic profile drag coefficient Ca for various craft (models)

Item	Craft name	Craft type	C_a	Source of data
1	SR.N2	ACV	0.25	ADAO 22583
2	SR.N4	ACV	0.30	ADAO 22583
3	SR.N5	ACV	0.38	ADAO 22583
4	SKMR.1	ACV	0.398	AIAA 73–318
5	SK–5	ACV	0.28	AIAA 73–318
6	JEFF(B)	ACV	0.495	AIAA 73–318
7	*Voyageur*	ACV	0.75	AIAA 73–318
8	N500	ACV	0.30	AIAA 73–318
9	SES-100B	SES	0.32	ADAO 22583
10	Model 719	SES	0.63	Maric Report

3.5 Aerodynamic momentum drag

Pressurized air has to be blown into the air cushion to replace air leakage out from the cushion under the skirt or seals in order to maintain the ACV/SES travelling on cushion. Thus, this mass of pressurized air contained in the cushion will be accelerated to the speed of the craft. The drag due to the momentum change of this air mass is called the aerodynamic momentum drag and can be calculated as

$$R_m = Q\rho_a v \tag{3.7}$$

where R_m is the aerodynamic momentum drag (N), Q the air inflow rate (m^3/s), ρ_a the air mass density (Ns^2/m^4) and v the craft speed (m/s). Q is generally calculated by including the cushion air inflow rate together with the air inflow rate for gas turbine intake systems and engine cooling systems.

3.6 Differential air momentum drag from leakage under bow/stern seals

According to momentum theory this drag can be written as

$$R_{\alpha''} = \rho_a (\phi h_1 B_c P - \phi h_2 B_c P)P \approx W\alpha'' \tag{3.8}$$

where $R_{\alpha''}$ is the air momentum drag from differential leakage under bow/stern skirts, ϕ the discharge coefficient of air leakage (in general we take $\phi = 0.5$–0.6), h_1 the bow air leakage clearance, i.e. the vertical distance between the lower tip of bow skirt/seal and the corresponding inner water-line, (m), h_2 the stern air leakage clearance (m), α'' the declined angle between the inner water line and the line linking the lower tips of the bow/stern seals, while the craft is travelling on the cushion (°), p_c the cushion pressure, (N/m^2) and $P = \sqrt{(2p_c/\rho_a)}$. From Fig. 5.12, $R_{\alpha''}$ can be written as

$$R_{\alpha''} = W/l_c\,[(z_b - t_{bi}) - (z_s - t_{si})] \tag{3.9}$$

where z_b, z_s are the vertical distances of the lower tip of bow/stern skirts over the craft base-line (m) and t_{bi}, t_{si} the vertical distance between the inner water line and the craft base-line (m). Because the z_b, z_s are given for the given craft and t_{bi}, t_{si} can be obtained by the equation listing in Chapter 5, $R_{\alpha''}$ can be obtained using equation (3.9).

$R_{\alpha''}$ relates to cushion length–beam ratio, Fr, and cushion pressure–length ratio (these parameters influence the profile of the inner wave surface), and the location of the centre of gravity (CG), (which influences the trim angle and inner/outer water line of the craft), as well as to z_b and z_s.

In order to reduce $R_{\alpha''}$, or to increase the jet thrust from a stern seal to increase craft speed, drivers can sometimes increase the stern seal clearance to make $R_{\alpha''}$ less than zero. In fact it is very difficult to predict this drag. According to the general custom of ACV designers and also for reasons of conservatism, we often take $\alpha'' = 0.25$–$0.5°$ for ACVs, and neglect this drag term for SES. This may be validated by prototype tests, in which a lot of spray will be seen behind the stern seal.

With the aid of Fig. 3.13, we can demonstrate this concept. In this figure, we have AB as the line linking the lower tip of the bow/stern seal (skirts), and ψ' the angle between sea level SL and AB. ψ' does not denote the trim angle of the craft, except if the line AB is parallel to the base-line of the craft. α' is the slope angle of the inner wave surface, and R_w the wave-making drag. From Fig. 3.13, we derive the following:

- When $\psi' > 0$, i.e. the craft operates with bow up, then

$$R_{\alpha''} = W \tan \psi' - R_w \tag{3.10}$$

If line AB is parallel to the base-line of the craft, then the drag due to the

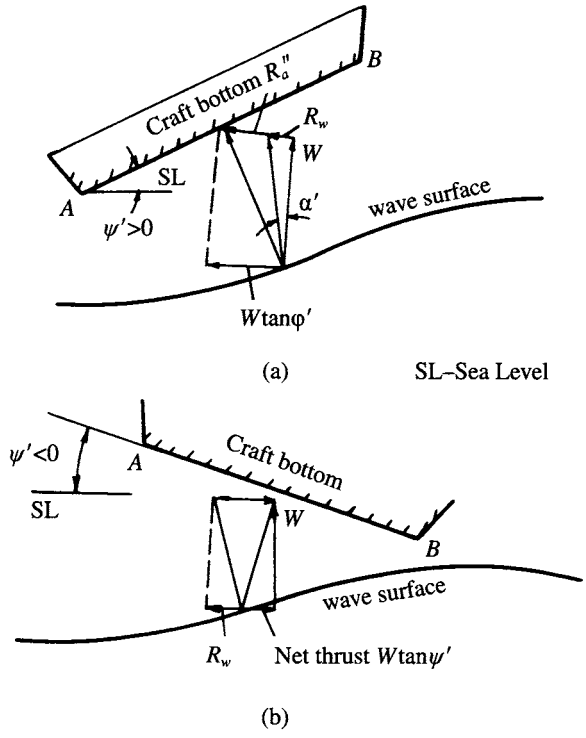

Fig. 3.13 Cushion wave-making drag and drag due to the difference of air momentum leaking from bow and stern of cushion.

differential air momentum leaking from the bow/stern skirts $R_{a''}$ is equal to the trim drag minus the wave-making drag.

- When $\psi' < 0$, i.e. the craft operates with bow down, then

$$R_{a''} = -W\tan\psi' - R_w < 0$$

which means $R_{a''}$ becomes a thrust and makes a net thrust of $W\tan\psi'$.

3.7 Skirt drag

The composition of skirt drag can be written as

$$R_{sk} = R_{sf} + R_{sp} + R_{ss} + R_{si}$$

where R_{sk} is the total skirt drag (N), R_{sf} the skirt water friction (N), R_{sp} the skirt pressure drag (N), R_{ss} the skirt spray drag (N) and R_{si} the skirt inertia drag (N).

R_{si} is the wave-making drag induced by the high frequency vibration of the skirt. For this reason, this drag is relative to the mass of the skirt, therefore this drag is also called inertia drag.

R_{sp} is the result of the cushion pressure and internal loads on the deformed part of the skirt above the water level locally balancing the water pressure acting on the part

of the skirt immersed in the water. The overall equilibrium between these forces within the whole skirt and R_{sp}, is the component along the x-direction L_s called skirt pressure drag.

Skirt drag not only relates to the immersion depth of skirts and spray making, but also the density of the skirt material. Therefore, it is very difficult to predict this drag by theoretical calculation; it can only be estimated with accuracy by full scale experimental methods or scaling from model test results.

Total skirt drag, R_{sk}

With respect to an ACV, skirt friction with the water surface is a large component of total drag, owing to the high density of water, 800 times larger than that of air.

Most of the skirt makes only slight contact with the water, while at the stern and the two stern corners of a skirt, segmented or fingered skirts may cause a large amount of scooping drag at lower speeds (particularly below hump speed, or $Fr < 0.75$). This can cause a particular problem for transiting hump speed if the skirt geometry is unfavourable. In addition the craft trim can strongly affect scooping. Above hump speed the skirt in the rear third of the craft is the most important for determining skirt drag in a steady condition. Normally the rear skirt lower tip is raised to minimize skirt drag.

Sometimes skirt drag will increase severely because of poor running trim, when either the bow skirt contacts the water surface (LCG too far forward) or the corners of the stern skirt scoop water (LCG too far back).

The skirt drag of a model tested in a towing tank will generally be less than that experienced at full scale, around 35% of total drag, as the running attitude of the craft can be regulated to be optimal. In contrast, the skirt drag for full scale craft will increase to about 55% or more of the total drag in the case of unfavourable craft trim. This drag level is generally not reproducible in the towing tank, so powering estimates for craft need to account for this difference.

A short description of each component is now given below.

Skirt friction drag, R_{sf}

We take the bag–finger type bow skirt or open loop type as an example to analyse the force exerted on the skirts and assume that the skirt fabric is perfectly flexible. That means the skirt fabric will be flattened and in close proximity to the water surface as the skirts make contact with the water surface as shown in Fig. 3.14; the deformation and applied force on the skirts can be expressed as in [24].

$$L_1 + L_2 = [d + R(1 - \cos\theta]/\sin\theta \tag{3.11}$$

where L_1 is the arc length of the part of the skirt in contact with the water surface (m), L_2 the flattening part of the skirt in close proximity to the water surface (m), R the radius of curvature due to the bending part of the skirt (m), d the immersion depth of the skirt (m) and θ the declination angle of the skirts, (°).

Meanwhile the water friction of the skirt balances with the tensions in the fabric, which can be written as

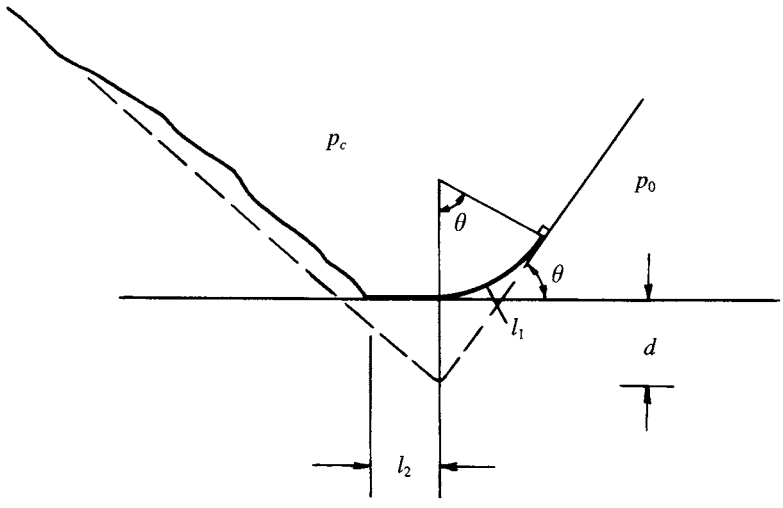

Fig. 3.14 Deflection of flexible skirts contacting water surface.

$$D = (p_c - p_0)R = p_c R = R_{sf}$$

where D is the tension of skirt fabric per unit width (N/m), p_c the cushion pressure (N/m^2), p_0 the atmospheric pressure and which equals zero and R_{sf} the water friction of the skirt per unit width (N/m).

Since the Reynolds number, Re is large for the skirt, the skirt fabric can be considered as a rough surface for friction, then

$$R_{sf} = 0.032\,(k/p_z)^{0.2} p_z\, q_w \tag{3.12}$$

in which k is the coefficient due to equivalent roughness and q_w the hydrodynamic pressure (N/m^2), $= 0.5\,\rho_w\, v^2$. Thus equation (3.11) can be written as

$$l_2 = \frac{d}{\sin\theta} + \frac{R_{sf}}{p_c}\left[\frac{1-\cos\theta}{\sin\theta} + \frac{\theta}{57.29}\right] \tag{3.13}$$

The values of R_{sf} and l_2 can be defined from equations (3.12) and (3.13), i.e. the two-dimensional equations. It is usual to assume that $d = l_2$ when calculating the wet surface of the skirt. In fact, this creates some errors due to neglecting the definite radius of curvature R, which is not equal to zero, but relative to the water friction and skirt fabric tension this is a small error. In the case of calculating the friction of stern skirts, the determination of the friction coefficient is in fact very complicated because the immersion depth of the stern skirt of a craft running over water is so small and it also makes a large amount of spray due to the pressure of the air cushion. Therefore, the problem becomes the drag concerned with the dynamics of two-phase flow – thus R_{sk} can be written as

$$R_{sk} = f\,(Re_j, \bar{Q}, d/p_c, W_e, F_{rl} \ldots) \tag{3.14}$$

where Re_j is the Reynolds number for jet air, $\bar{Q}$ the flow rate coefficient, which affects the spray, W_e the Weber number $= \rho_w\, v_j^2\, t/\sigma_t$ which also affects the initiation of spray,

V_j the jet velocity from the stern cushion, t the thickness of the jet from the stern cushion and σ_t the surface tension of water.

The water friction of the stern skirt will decrease due to two-phase flow through the gap under the segment tips or bag lower point, since the turbulent air flow creates dense spray.

Skirt pressure drag, R_{sp}

This may be written as

$$R_{sp} = (p_c - p_0)\mathrm{d} = p_c\mathrm{d} \tag{3.15}$$

As mentioned above, the various components of skirt drag, such as friction drag in two-phase flow, the inertia drag of the skirt due to the flutter of the skirt fabric and spray drag of skirts at both sides of the craft, are difficult to calculate. For this reason, the total skirt drag is best estimated by experience-based formulae [25, 26], as follows:

$$R_{sk} = R_{sk1} + R_{sk2} \tag{3.16}$$

$$R_{sk1} = C_{sk1} \times 10^{-6}(h/l_j)^{-0.34}\, l_j\, S_c^{0.5}\, q_w \tag{3.17}$$

$$R_{sk2} = C_{sk2} R_w \tag{3.18}$$

$$C_{sk2} = \{[2.8167\,(p_c/l_c)^{-0.259}] - 1\}$$

where R_{sk} is the skirt total drag, R_{sk1} the wet drag of the skirt, R_{sk2} the wave-making drag due to the skirt, h the average clearance for air leakage where $h = S_j/l_j$ in static hovering mode, where S_j denotes the area of air leakage under the skirts, l_j the total peripheral length of the skirts, including the delta area for air leakage at the tip of finger in the case of using bag and finger type skirts, R_w the wave-making drag due to the air cushion, S_c the cushion area, q_w the hydrodynamic head due to craft speed $= 0.5\,\rho_w\, v^2$, C_{sk1} the coefficient for hydrodynamic drag, $C_{sk} = 2.5$–3.5 or $[1.35 + 0.112\,p_c/l_c]$, and C_{sk2} the coefficient due to wave-making drag of the skirt, obtained by equation (3.16) or Fig. 3.15.

These equations were obtained from model experimental data. In fact equation (3.17) can be written as

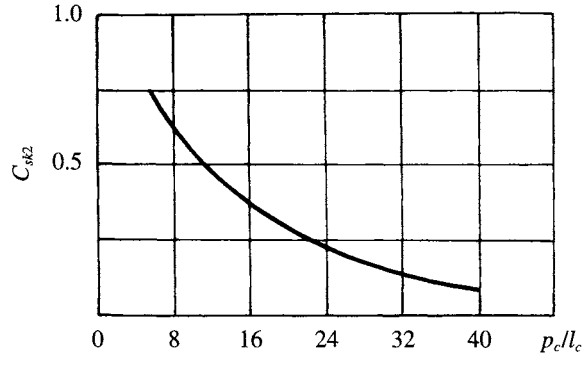

Fig. 3.15 Variation of skirt wave-making drag coefficient C_{sk2} with cushion length/beam ratio P_c/L_c.

$$R_{sk1}/W = C_{sk1} \times 10^{-6} (h/l_j)^{-0.34} l_j/p_c \, q_w/S_c^{0.5} \tag{3.18a}$$

where W is the weight of the craft (N).

Drag of bow/stern seals of an SES, R_{sb}, R_{ss}

This is also estimated based on test data. Two methods for predicting this drag are as follows.

MARIC method [27]

Based upon a series of model tests, a statistical analysis was carried out at MARIC. Putting the skirt (bow/stern) drag, the drag due to the differential momentum from the bow/stern seals, the wave-making drag of sidewalls, and the interference drag due to sidewalls, all into a single term 'residual drag' and then processing this by regression analysis, the following equation is obtained:

$$R_r = C_r' \, B_c \, h_c \, q_w \tag{3.19}$$

where R_r is the residual drag of an SES (N), C_r' the residual drag coefficient and h_c the water surface depression induced by air cushion pressure.

C_r' may be obtained from Fig. 3.16. An intermediate value might be chosen. The lower value relates to the better performing seals (making the flow of air leakage under the stern seal significantly larger than that under the bow seal), and the better running attitude of the craft. In contrast, the larger value relates to a skirt with no designed rear gap at level trim, or the craft trim being more bow up, for example due to a service requirement for open sea conditions rather than coastal or protected waters.

This experimental expression is based upon the following conditions:

$$l_c/B_c = 3.5\text{–}4.0 \qquad p_c/l_c = 15\text{–}18.5 \text{ kgf/m}^3 \qquad 0.7 < Fr_l < 1.2$$

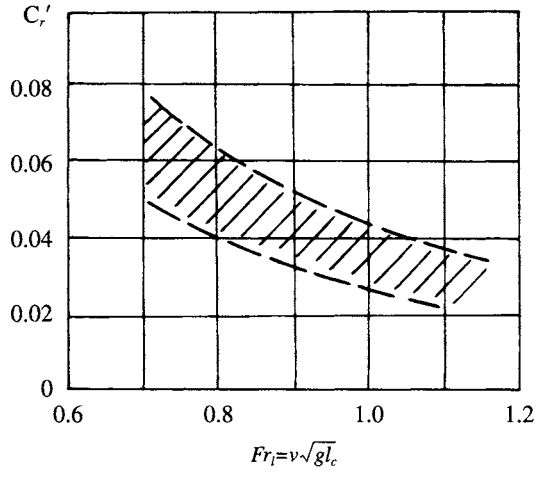

Fig. 3.16 Variation of seal drag coefficient C_r' with Froude Number.

Rin-Ichi Marao method [28]

Model experiments were carried out on an SES with thin plates as sidewalls and with $l_c/B_c = 2$ approximately, by Rin-Ichi and Marao. The air profile drag was then deducted and the aerodynamic momentum drag and wave-making drag obtained from analysis of the measured wave profile. These components were then deducted from the total drag of models to obtain the residual drag. The form drag of sidewalls can be neglected due to the thin plate sidewalls used, so that the residual drag can be approximated directly to the seal drag and written as

$$R_{sk} = C_{sk}\ B_c\ h_c\ q_w \tag{3.20}$$

where R_{sk} is the seal drag of an SES, C_{sk} the coefficient for skirt (seal) drag, as shown in Fig. 3.17 and q_w the hydrodynamic head of the craft at speed.

B. A. Kolezaev method

From reference 19, expressions for skirt drag can be written as

$$R_{sk} = (a + b\ Fr_d)\ B_c\ p_c\ v \tag{3.21}$$

where Fr_d is the Froude number due to the volumetric displacement,

$$Fr_d = v/(g\ D^{0.33})^{0.5}$$

and D is the volumetric displacement of the craft (m^3), a the experimental coefficient, $0.00225 \leqslant a \leqslant 0.021$, b the experimental or experience coefficient, $0.0015 \leqslant b \leqslant 0.0087$ and v the velocity (m/s). Coefficients a and b are dependent upon the material configuration and aerodynamic performance of the seals.

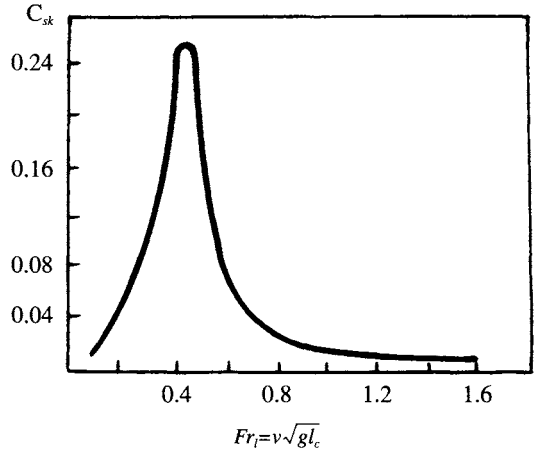

Fig. 3.17 Seal drag coefficient vs Froude Number at optimum trim angle.

3.8 Sidewall water friction drag

Friction drag is a large proportion (up to 30–40% for high speed craft) of total craft drag, as shown in Fig. 3.1. For this reason, calculation has to be made carefully. The main difficulty is to determine the wetted surface accurately.

In general, two methods are used: one is the theoretical method as described in Chapter 5 and the other is a model experimental method similar to that used in planing hull design, i.e. the wetted area can be obtained by photographs. We will introduce four different practical methods for predicting the wetted surface by experimental and statistical analysis methods.

With respect to the sidewall water friction drag, the following equation can be used:

$$R_{swf} = (C_f + \Delta C_f)\, S_f\, q_w \tag{3.22}$$

where R_{swf} is the water friction drag of sidewalls (N), C_f the coefficient for the friction of the plate, obtained by $0.455/[l_s\, Re]^{2.58}$ (3.23), ΔC_f the coefficient due to added roughness of the sidewalls, between 0.3 and 0.4×10^{-3}, Re the Reynolds number $= l_s v_s/\upsilon$, l_s the wetted length of sidewalls (m), v_s the craft speed, (m/s^2), υ the kinematic viscosity coefficient (m^2/s) and S_f the wetted surface of the craft running on the cushion (m^2).

MARIC method [29]

The sidewall wetted surface is dependent upon craft trim. It is subsequently a function of wave-making generated by the air cushion, the sidewalls and their interference with each other, lift system characteristics, as well as the seal clearance over the base line of the craft, etc. The theoretical method for prediction is therefore complicated. For this reason, the simplest way to predict the wetted surface area may be by means of measurement from photographs.

Figure 3.18(a) shows the outer surface of an SES model running at below hump speed (Fr = 0.239), Fig. 3.18(b) shows that above hump speed (Fr = 2.15) and Fig. 3.19 shows the added wave-making due to the bow seal pushing water (described in detail in the following paragraphs of this chapter). Thus, the curve showing the relation between the wetted surface of inner/outer sidewalls and the Fr can be obtained by the photographic method from model experiments.

Then the wetted surface of sidewalls of craft running on cushion can be written as

$$S_f = K_i\, S_{i0} + K_{out}\, S_{out0} \tag{3.24}$$

where K_i, K_{out} are correction coefficients for the inner/outer wetted surface of sidewalls, which can also be written as

$$K_i = S_i/S_{i0}$$

$$K_{out} = S_{out}/S_{out0}$$

These coefficients can be determined by photographs or experimental results from similar craft models. Also S_{io}, S_{out0} are the wetted inner/outer surface breadth of sidewall of craft hovering static (Fig. 3.20) (m) and S_i, S_{out} the wetted inner/outer surface area of sidewall of craft running on the cushion.

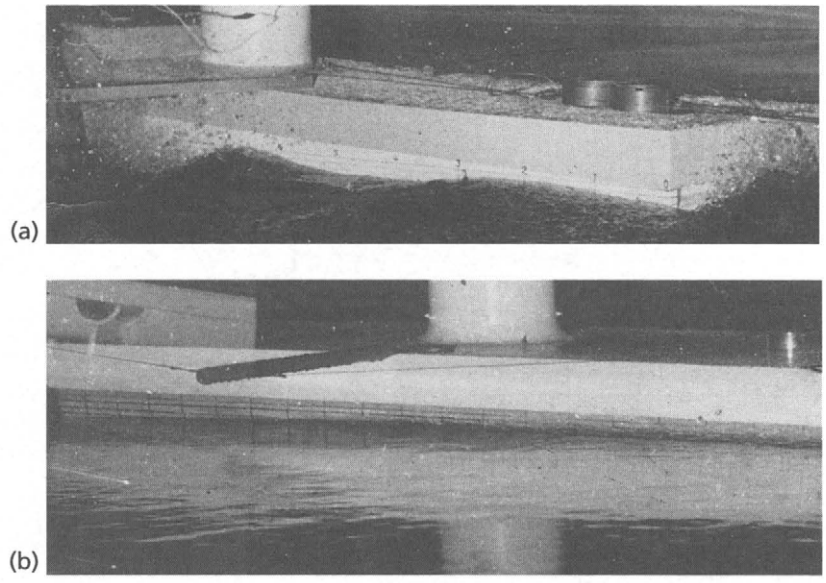

Fig. 3.18 Running attitude of SES model on cushion: (a) $F_r = 0.239$ (during take-off); (b) $F_r = 2.15$ (post take-off).

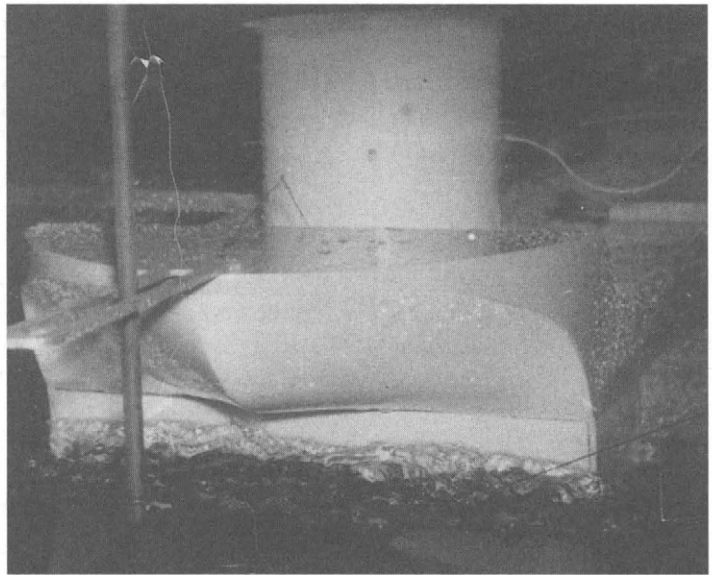

Fig. 3.19 Water contact phenomenon of bow seal during take-off.

Owing to the smaller inner wetted surface area by comparison with the outer one and also the difficulty in photographing the inner wetted surface, the total area of wetted surface is estimated as

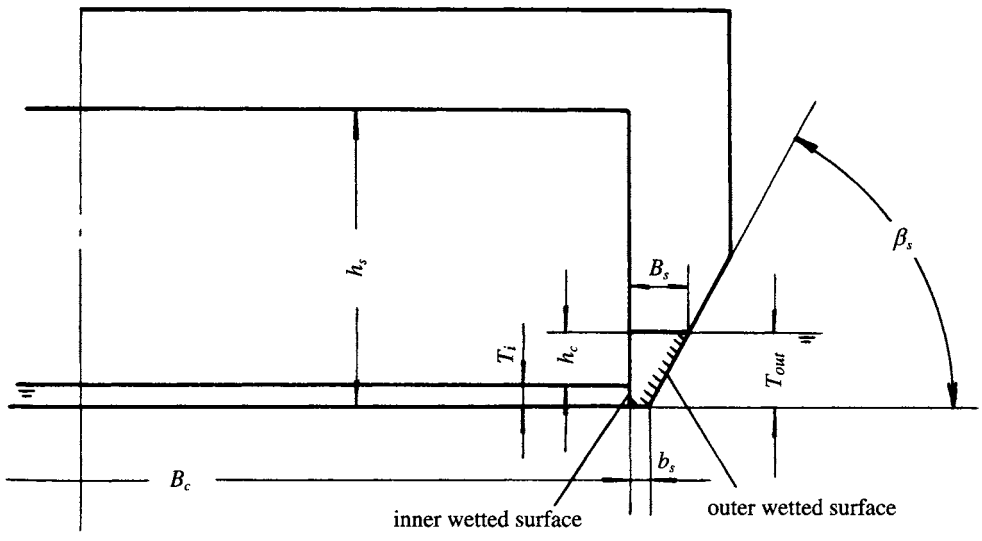

Fig. 3.20 Sketch of wetted surface of SES.

$$S_f = S_{i0} + S_{out0} K_{out} \tag{3.25}$$

where K_{out} can be obtained from Fig. 3.21, which has been obtained by statistical analysis of photographs on model no. 4 by MARIC. It is found that there are two hollows on the curve of the outer wetted surface area, the first is due to the hump speed, which leads to a large amount of air leakage amidships, and the second is caused by small trim angle at higher craft speed.

Method used in Japan [28]

Reference 28 introduces the measurement of the inner/outer wetted surface area of a plate-like sidewall of an SES with cushion length beam ratio (l_c/B_c) of about 2 on the cushion and represented as follows (Fig. 3.22):

$$S_f = S_{f\infty} + (S_{f0} - S_{f\infty})\, e^{-Fr} + 4h_c\, l_s f_s \tag{3.26}$$

where S_f is the area of the wetted surface of sidewalls (m^2), $S_{f\infty}$ the area of the wetted surface of sidewalls at high speed (m^2) and f_s the correction coefficient for the area of the wetted surface, which can be related to Fr_l, as shown in Fig. 3.23 and which is obtained by model test results.

In the case of craft at very high speed (higher than twice hump speed), the water surface is almost flat at the inner/outer wave surface and also equal to each other. With respect to the rectangular transverse section of the sidewalls, the wetted area can be written as

$$S_{f\infty} = [4(h_2 - h_{eq}) + 2\, B_s]\, l_s \tag{3.27}$$

S_{f0} is the wetted surface area of the sidewalls of craft hovering statically (m^2),

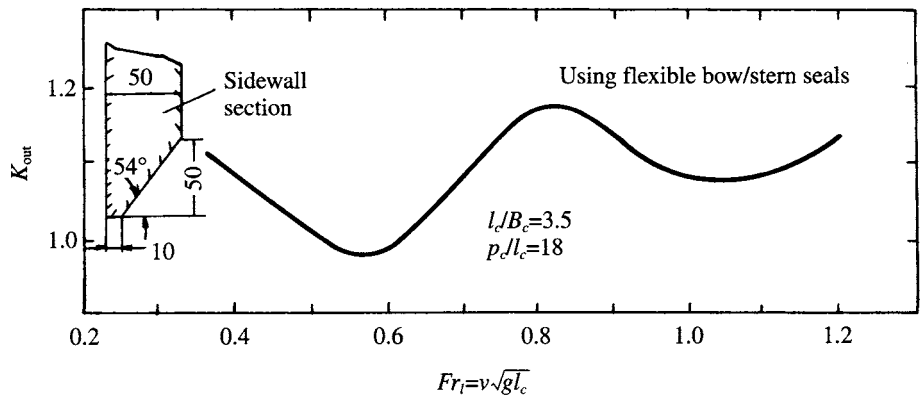

Fig. 3.21 Correction coefficient of outer wetted surface area of SES with flexible bow/stern seals.

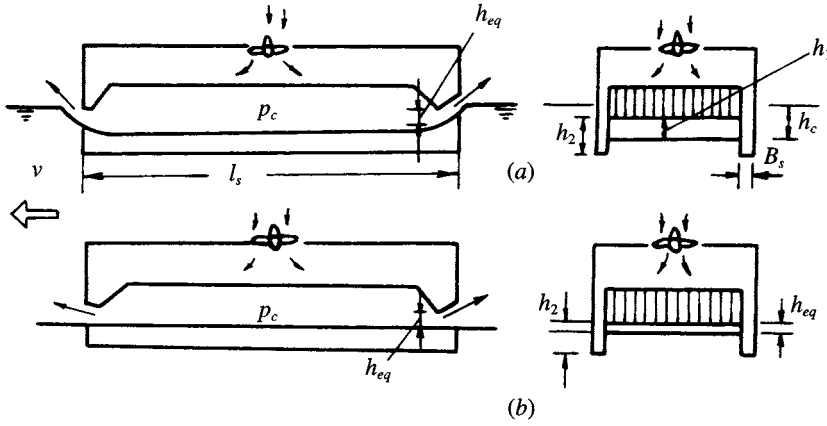

Fig. 3.22 Sketch of SES running attitude at F_r = 0(a) and F_r = 00(b).

$$S_{f0} = [4(h_2 - h_1) + 2\,h_c + 2\,B_s]\,l_s$$
$$= 4\,[T_i + 2\,h_c + 2\,B_s]\,l_s \tag{3.28}$$

where B_s is the width of the sidewalls with rectangular transverse section (m), l_s the length of sidewalls (m), h_c the depth of cushion air water depression, hovering static (m), h_1 the vertical distance between the lower tip of skirts and inner water surface, i.e. $h_1 = h_2 - T_i$, as shown in Fig. 3.24, hovering static (m), h_2 the vertical distance between the lower skirt tip and craft baseline (i.e. z_b, z_s, in Chapter 5) (m), T_i the inner sidewall draft, hovering static, and h_{eq} the equivalent air gap,

$$h_{eq} = Q/(l_j\,(2p_c/\rho_a)^{0.5})$$

where Q is the cushion flow rate (m^3/s), p_2 the cushion pressure (N/m), ρ_a the air density (Ns^2/m^4), l_j the total length of air leakage at the bow/stern seal (m) and B_c the cushion beam (m).

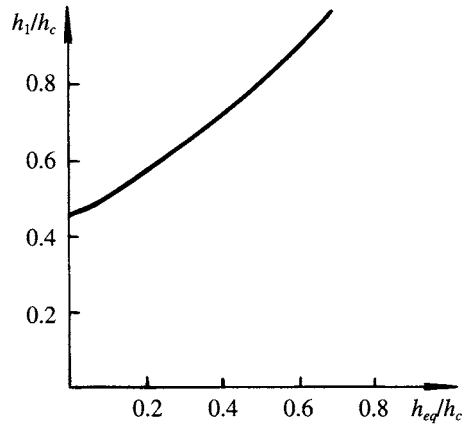

Fig. 3.23 Equivalent leakage h_{eq} compared to the distance from seal lower edge to the cushion inner water surface.

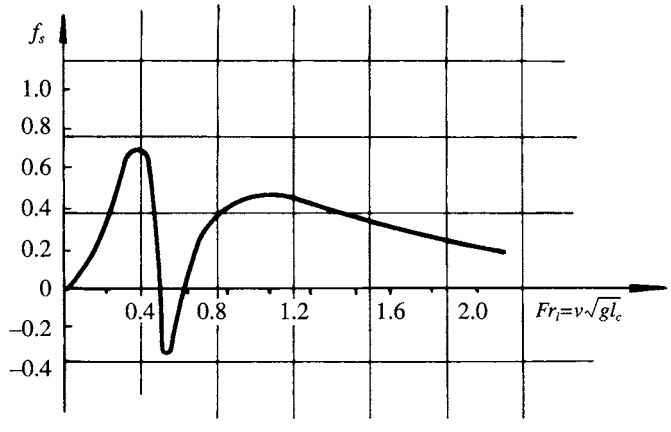

Fig. 3.24 Correction coefficient for sidewall wetted surface area.

From equations (3.27) and (3.28) the area of wetted surface at any given Fr_1, can be interpolated from

$$\text{at } Fr_1 = 0, \qquad S_f = S_{f0} \text{ (max. area of wetted surface)}$$

$$\text{at } Fr_1 = \infty \qquad S_f = S_{f\infty} \text{ (min. area of wetted surface)}$$

and

$$S_{f\infty} < S_f < S_{f0}$$

NPL method (The UK National Physical Laboratory) [15]

Based on model tests in their towing tank, the following method was obtained by NPL:

$$S_f = (S_{f0} + \Delta S_f)(1 + 5\, B_{smax}/l_s) \tag{3.29}$$

where B_{smax} is the max. width of sidewalls at design water line (m), ΔS_f the area correction to the wetted surface due to the speed change (m^2) and S_{f0} the area of wetted surface of sidewalls during static hovering (m^2).

This expression is suitable for the following conditions:

$$8 < p_c/l_c < 16 \quad \text{and} \quad Fr_l \geq 1.2$$

Figure 3.25 shows a plot enabling ΔS_f to be determined within these conditions.

B. A. Kolezaev method (USSR) [19]

B. A. Kolezaev derived the following expression for sidewall drag:

$$S_f = K_f\, S_{f0}$$

where S_f is the area of wetted surface, hovering static (Fig. 3.26), K_f the correction coefficient for the wetted surface, related to Fr (Fig. 3.27). S_{f0} can also be written as below (see Fig. 3.26):

$$S_{f0} \approx 2l_s\left[T_i + T_o + b_s + (B_s - b_s)\left(1 - \frac{\sin\beta}{\cos\beta}\right)\right] \tag{3.30}$$

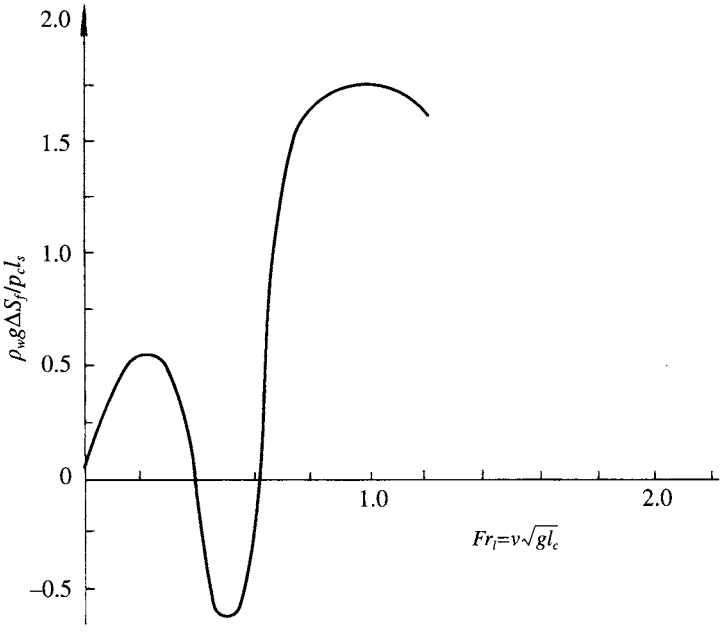

Fig. 3.25 Correction coefficient of wetted surface area of sidewall vs Froude Number. [15]

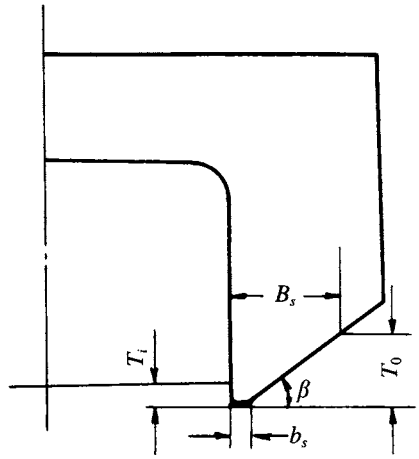

Fig. 3.26 Typical dimensions for wetted surface of sidewalls.

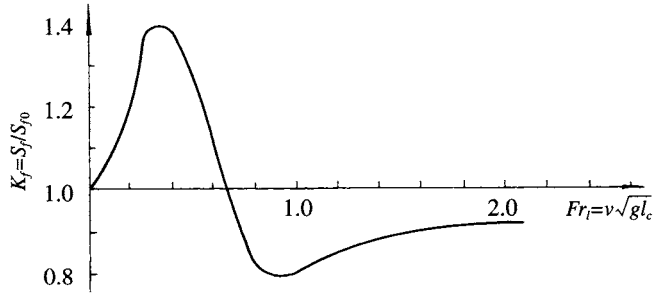

Fig. 3.27 Correction coefficient of wetted surface area of sidewalls vs Froude Number.

where T_i, T_o are the inner/outer drafts, hovering static (m), b_s the width of the base plate of the sidewalls (m), B_s the width of sidewalls at designed outer draft (m) and β the deadrise angle of sidewalls (°).

A number of methods used for predicting the area of the wetted surface have been illustrated in this section. It is important to note that one has to use these expressions consistently with expressions by the same authors to predict the other drag components, such as skirt drag, residual drag, etc., otherwise errors may result.

As a general rule, the methods derived from model tests and particularly photo records from the actual design or a very similar one will be the most accurate. The different expressions may also be used to give an idea of the likely spread of values for the various drag components during the early design stage.

3.9 Sidewall wave-making drag

Equivalent cushion beam method

SES with thin sidewalls create very little wave-making drag, owing to their high length/beam ratio, which may be up to 30–40. To simplify calculations this drag may be included in the wave-making drag due to the air cushion and calculated altogether, i.e. take a equivalent cushion beam $\bar{B}_c$ to replace the cushion beam B_c for calculating the total wave drag. Thus equation (3.1) may be rewritten as

$$R_w = \bar{C}_w p_c^2 \bar{B}_c/(\rho_w g) \tag{3.31}$$

where R_w is the sum of wave-making drag due to the cushion and sidewalls, $\bar{C}_w$ the coefficient of wave-making drag, $C_w = f(Fr_l, l_c/\bar{B}_c)$ and $\bar{B}_c$ the equivalent beam of air cushion including the wave-making due to the sidewalls.

The concept of equivalent cushion beam can be explained as the buoyancy of sidewalls made equivalent to the lift by an added cushion area with an added cushion beam. The cushion pressure can be written as

$$p_c = (W - W_s)/(l_c B_c)$$

where W_s is the buoyancy provided by sidewalls and W the craft weight. Then the equivalent cushion beam can be written as

$$\bar{B}_c = \frac{W}{p_c l_c} = \frac{W}{[(W - W_s)/(l_c B_c)]\, l_c} = \frac{B_c}{1 - W_s/W} \tag{3.32}$$

The method mentioned above has been applied widely in China by MARIC to design SES with thinner sidewalls and high craft speed and has proven accurate. Following the trend to wider sidewalls, some discrepancies were obtained between the calculation and experimental results. For this reason, [29] gave some discussion of alternative approaches.

Equation (3.31) can be rewritten by substitution of (3.32) into (3.31), as

$$R_w = \left[\frac{C_w p_c^2 B_c}{\rho_w g}\right] \cdot \left[\frac{\bar{C}_w}{C_w}\right] \cdot \left[\frac{\bar{B}_c}{B_c}\right]$$

$$= \frac{\bar{C}_w}{C_w} \cdot \frac{R_{wc}}{1 - W_s/W} \tag{3.33}$$

Where R_{wc} is the wave-making drag caused by the air cushion with a beam of B_c and without the consideration of wave-making drag caused by sidewalls, $\bar{C}_w$ the coefficient due to the wave-making drag with respect to Fr, $l_c/\bar{B}_c$

$$\bar{C}_w = f\,(Fr_l, l_c/\bar{B}_c)$$

and C_w the coefficient due to the wave-making drag with respect to Fr, l_c/B_c

$$C_w = f\,(Fr_l, l_c/B_c)$$

The total wave-making drag of SESs can now be written as

$$R_w = R_{wc} + R_{sww} + R_{wi} \tag{3.34}$$

where R_{wc} is the wave-making drag caused by the air cushion, R_{sww} the wave-making drag caused by the sidewalls and R_{wi} the interference drag caused by the air cushion and sidewalls. Therefore

$$R_{sww} + R_{wi} = R_w - R_{wc} \tag{3.35}$$

as

$$R_{wc} = C_w \, p_c^2 \, B_c/(\rho_w g) \tag{3.36}$$

and

$$p_c = W - W_s/(l_c \, B_c)$$

Therefore

$$R_{wc} = [C_w \, B_c/(\rho_w g)] \; [W - W_s/(l_c \, B_c)]^2 \tag{3.37}$$

If we substitute equations (3.36) and (3.33) into (3.35), we obtain

$$R_{sww} + R_{wi} = \frac{\bar{C}_w}{C_w} \; \frac{R_{wc}}{1 - W_s/W} - R_{wc}$$

$$= R_{wc} \left[\frac{\bar{C}_w}{C_w} \; \frac{1}{1 - W_s/W} \right] - 1 \tag{3.38}$$

If R denotes the buoyancy of sidewalls and equals zero, then the whole weight of the craft will be supported by the air cushion with an area of S_c ($S_c = l_c \, B_c$) and the wave-making drag could then be written as

$$R_{wc0} = [C_w \, B_c/(\rho_w g)] \; [W/(l_c \, B_c)]^2 \tag{3.39}$$

From equations (3.37) and (3.39) we have

$$R_{wc}/R_{wc0} = (1 - W_s/W)^2 \tag{3.40}$$

Upon substitition of equation (3.40) in (3.38) and using equation (3.39), then equation (3.38) can be written as

$$R_{sw} + R_{wi} = R_{wc0} \, [(\bar{C}_w/C_w) \, (1 - W_s/W) - (1 - W_s/W)^2] \tag{3.41}$$

The calculation results are shown in Fig. 3.28. It can be seen that the less the W_s/W, the less the wave-making drag of the sidewalls ($R_{sww} + R_w$), which is reasonable. The greater the W_s/W, the more the wave-making drag of the sidewalls.

Figure 3.28 also shows that wave-making drag decreases as the W_s/W exceeds 0.5. This seems unreasonable. The calculation results of [30] and [31] showed that wave-making drag will increase significantly as W_s/W increases. Reference 32 also showed that the wave-making drag of sidewalls could be neglected in the case of $W_s/W <$ 15%.

The equivalent cushion beam method is therefore only suitable to apply to SES with thinner sidewalls. It is unreasonable to use this method for SES with thick sidewalls or for air cushion catamarans (e.g. $W_s/W \approx 0.3$–0.4) and for these craft the wave-making drag of sidewalls has then to be considered separately.

Yim [30] calculated the wave-making drag due to sidewalls by means of an even simpler method. He considered that the total wave-making of an SES would be equal to that of an ACV with the same cushion length and beam, i.e. it was considered that the sidewalls did not provide any buoyancy, and the total craft weight would be supported only by an air cushion as to lead the same wave-making due to this equivalent air cushion. The effective wave-making drag coefficient of the sidewalls calculated by this method is similar to that for $W_s/W > 0.5$ above (see Fig. 3.28).

Hiroomi Ozawa method [31]

The theoretical calculation and test results of the wave-making drag of air cushion catamarans have been carried out by Hiroomi Ozawa [31]. Based on rewriting his equations found in [29], the final equation for predicting total wave-making drag may be written as (when $Fr = 0.8$)

$$R_w = R_{ws} + R_{sww} + R_{wi} \tag{3.42}$$

$$R_w = [1 - 0.96\, W_s/W + 0.48\, (W_s/W)^2]\, [C_w\, B_c/(\rho_w\, g)]\, [W/(l_c\, B_c)]^2$$

A comparison between the equivalent cushion beam method, the Ozawa method and the Yim method is shown in Fig. 3.28. It can be seen that satisfactory accuracy can be

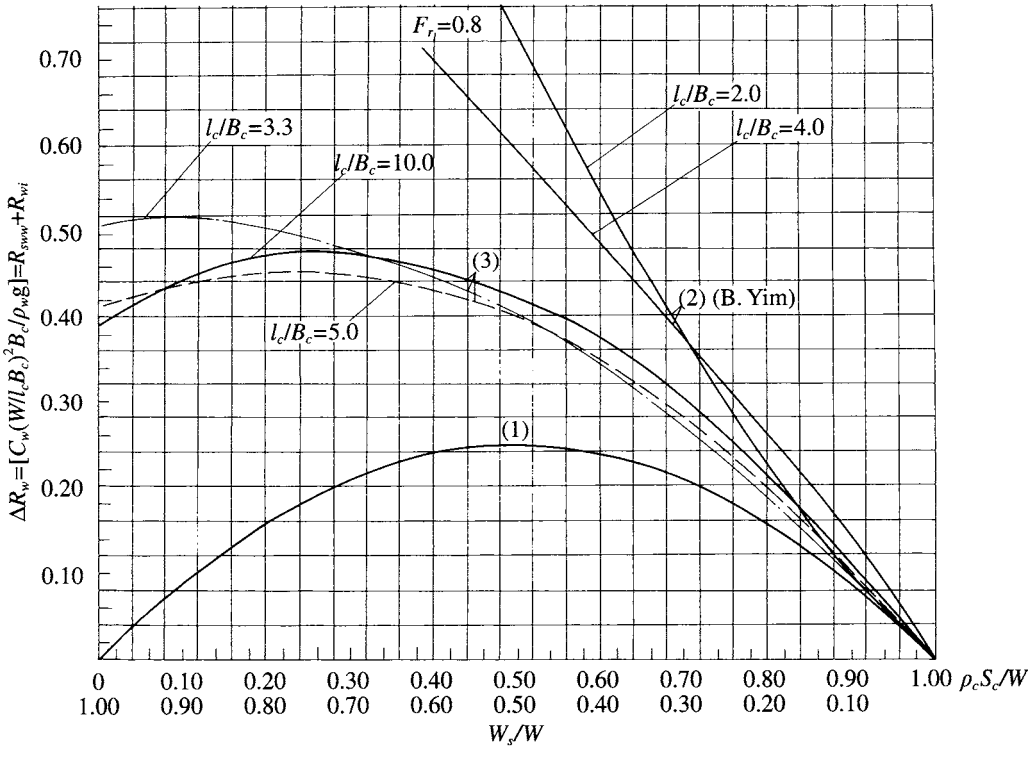

Fig. 3.28 Comparison of calculations for sidewall wave-making drag by means of various methods.

obtained by the equivalent method in the case of $W_s/W < 0.2$, but the wave-making drag of sidewalls and its interference drag with the air cushion have to be taken into account as W_s/W increases.

In conclusion, the methods for estimating sidewall drag introduced here are suitable for SES with sidewall displacement up to about 30% of craft total weight. Where a larger proportion of craft weight is borne by the sidewalls, the sidehull wave-making should be considered directly, rather than as a 'correction' to the cushion wave-making. Below 70% contribution to support from the air cushion, the beneficial effect of the cushion itself rapidly dies away, and so it is more likely that optimizing catamaran hulls will achieve the designer's requirements in the speed range to 40 knots. Above this speed, an air cushion supporting most of the craft weight is most likely to give the optimum design with minimum powering.

Calculation method for parabola-shaped sidewalls [33]

In the case where the sidewall water lines are slender and close to parabolic shape, then the wave-making drag of sidewalls can be written as

$$R_{sww} = C_{sww} (8 \rho_w g/\pi) (B_s^2 T_o^2/l_s) \tag{3.43}$$

where R_{sww} is the wave-making drag of the sidewall (N), C_{sww} the wave-making drag coefficient (Fig. 3.29), ρ_w the density of water (Ns^2/m^4), B_s the max. width of sidewalls (m) and T_o the outer draft of sidewalls (m).

B. A. Kolezaev method [19]

Kolezaev defined the residual drag of sidewalls as a function of craft weight:

$$R_{sww} = K_{fr} W$$

where R_{sww} is the residual drag of sidewalls (N), K_{fr} the coefficient of sidewall residual drag, obtained from Fig. 3.30, and W the craft weight (N).

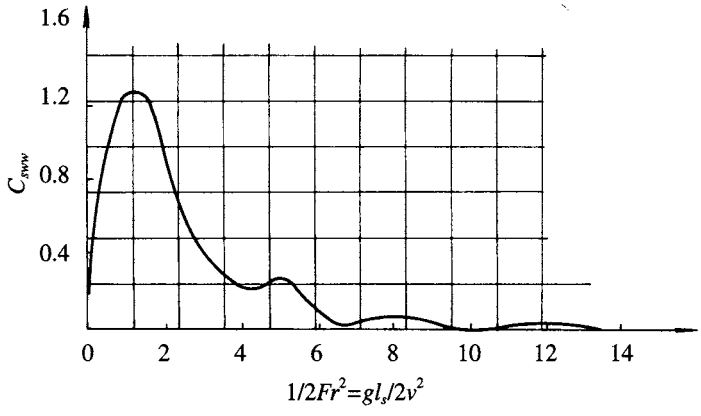

Fig. 3.29 Wave-making drag coefficient of slender sidewalls with the parabolic water planes. [39]

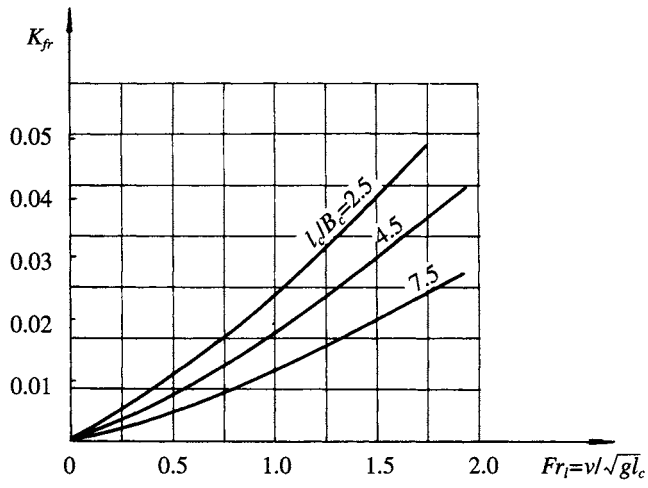

Fig. 3.30 Residual drag coefficient of sidewall as a function of L_c/B_c and Froude number.

3.10 Hydrodynamic momentum drag due to engine cooling water

In general, the main engines mounted on SES have to be cooled by sea water which is ingested from Kingston valves or sea water scoops mounted at propeller brackets, via the cooling water system, then pumped out from sidewalls in a transverse direction. The hydrodynamic momentum drag due to the cooling water can be written as

$$R_{mw} = \rho_w V_j Q_w \tag{3.44}$$

where R_{mw} is the hydrodynamic momentum drag due to the cooling water for engines (N), V_j the speed of inlet water, in general it can be taken as craft speed (m/s), and Q_w the flow rate of cooling water (m/s).

3.11 Underwater appendage drag

Drag due to rudders, etc.

Drag due to rudders and other foil-shaped appendages, such as plates preventing air ingestion, propeller and shafts brackets, etc. can be written as [34]:

$$R_r = C_{fr}(1 + \delta v/v)^2 (1 + r) S_r q_w \tag{3.45}$$

where R_r is the drag due to the rudder and foil-shaped propeller and shaft brackets (N), C_{fr} the friction coefficient, which is a function of Re and the roughness coefficient of the rudder surface. In this case $Re = (vc/v)$ where c is the chord length of rudders or other foil-like appendages (m), $\delta v/v$ is the factor considering the influence of propeller wake:

$\delta v/v = 0.1$ in general, or

$\delta v/v = 0$ if no effect of propeller wake on this drag;

v is craft speed (m/s), r the empirical factor considering the effect of shape, $r = 5\ t/c$, where t is foil thickness, S_r the area of wetted surface of rudders or foil-like appendages (m^2) and q_w the hydrodynamic head due to craft speed.

This equation is suitable for rudders or other foil-shaped appendages totally immersed in the water.

Drag of shafts (or quill shafts) and propeller boss [35]

This drag can be written as :

$$R_{sh} = C_{sh}\,(d_1\,l_1 + d_2\,l_2)\,q_w \tag{3.46}$$

where R_{sh} is the drag of the shaft (or quill shaft) and boss (N), d_1 the diameter of the shaft (or quill shaft) (m), d_2 the diameter of the boss (m), l_1 the wetted length of shafts (quill shaft) (m), l_2 the wetted length of the boss (m) and C_{sh} the drag coefficient of the shaft (quill shaft) and boss. For a perfectly immersed shaft (quill shaft) and boss and $5.5 \times 10^5 > R_{e_m} > 10^3$, then it can be written:

$$C_{sh} = 1.1 \sin^3\beta_{sh} + \pi\, Cf_{sh} \tag{3.47}$$

where β_{sh} is the angle between the shaft (quill shaft), boss and entry flow (for stern buttocks), Cf_{sh} the friction coefficient, which is a function of R_{e_m}, where

$$R_{e_m} = v\,(l_1 + l_2)/\upsilon$$

and also includes the roughness factor; for example, if $\beta_{sh} = 10°–12°$, with the shafts (quill shafts) immersed perfectly in water, then we take $Cf_{sh} = 0.02$.

Drag of strut palms

According to ref. 34, the drag of strut palms can be written as

$$R_{pa} = 0.75 C_{pa}\,(h_p/\delta)^{0.33}\,y\,h_p\,(\rho_w/2)\,v^2 \tag{3.48}$$

where R_{pa} is the drag of strut palms (N), y the width of strut palms (m) and δ the thickness of the boundary layer at the strut palms:

$$\delta = 0.016 x_p\ (\text{m})$$

where x_p is the distance between the stagnation point of water line and strut palms (m), h_p the thickness of strut palms (m) and C_{pa} the drag coefficient of strut palms, $C_{pa} \cong 0.65$.

Drag of non-flush sea-water strainers

According to ref. 34, the drag of non-flush sea-water strainers can be written as

$$R_0 = S_0\,C_0\,(\rho_w/2)\,v^2 \tag{3.49}$$

where R_0 is the drag due to non-flush sea-water strainers (N), S_0 the frontal projected

area of the sea-water inlet (m), C_0 the drag coefficient due to sea-water strainers, and v the craft speed (m/s).

There are a number of methods for predicting the appendage drag. In this respect, there is no difference between the appendages of SES and planing hulls, or displacement ships: the data from these can therefore be used for reference.

3.12 Total ACV and SES drag over water

Different methodologies to calculate the total drag of ACV/SES have been compiled and compared at MARIC [27]. Three methods for ACVs and five methods for SES may be recommended, as summarized below.

ACV

The calculation methods are shown in Table 3.2. Notes and commentary are as follows:

- It is suggested that method 1 can be used at design estimate or initial design stage. Since many factors cannot be taken into account at this stage, the method is approximate, taking a wide range of coefficients for residual drag. Method 3 is still approximate, although more accurate than method 1. For this reason it can be applied at preliminary design stage. With respect to method 2, it is suggested using this at detail design or the final period in preliminary design, because the dimensions in detail and the design of subsystems as well as the experimental results in the towing tank and wind tunnel should have been obtained.
- The drag for above-water appendages (air rudders, vertical and horizontal fins,

Table 3.2 Methods for calculating ACV over water drag

Drag components	Method 1 Estimation	Method 2 Conversion from model tests	Method 3 Interpretative
Aerodynamic profile drag		$R_a = 0.5\rho_a C_a S_a v^2$	
Aerodynamic momentum drag		$R_m = \rho_a Q v$	
Momentum drag due to differential leakage from bow and stern skirts		$R_w = C_w p_c^2 B_c/(\rho_w g)$	C_w can be obtained from Figs 3.2 and 3.3
Wave-making drag	$R_{\alpha''} = W\alpha''$	$R_{\alpha''}$ is included in R_r	$R_{\alpha''} = W\alpha''$
Skirt drag or residual drag	$R_s = (0.5 \sim 0.7)(R_a + R_m + R_w + R_{\alpha''})$	$R_r = (R_{tm} - R_{am} - R_{mm} - R_{wm})(W/W_m)$	$R_{sk} = C_{sk1} \times 10^{-6}(h/l_j)^{-0.34} l_j q_w S_c^{0.5} + \{[2.8167 (p_c/l_c)^{-0.259}] - 1\} R_w$ $C_{sk1} = 1.35 + 0.112 P_c/l_c$
Total drag	$R_T = K_T(R_a + R_m + R_w + R_{\alpha''})$ where $K_T = 1.5 \sim 1.7$	$R_T = R_a + R_m + R_w + R_r$	$R_T = K'_T(R_a + R_m + R_w + R_{\alpha''} + R'_{sk})$
Remarks	See Note 1	See Note 1	See Note 2

Note 1: In methods 1 and 3 α'' denotes the angle between the inner water surface and the line linking the lower tips of bow and stern skirts.

Note 2: In method 3, normally $K'_T = 1.15$–1.25, but where a large amount of references and experimental data are available, then K'_T may be reduced to 1.0–1.1.

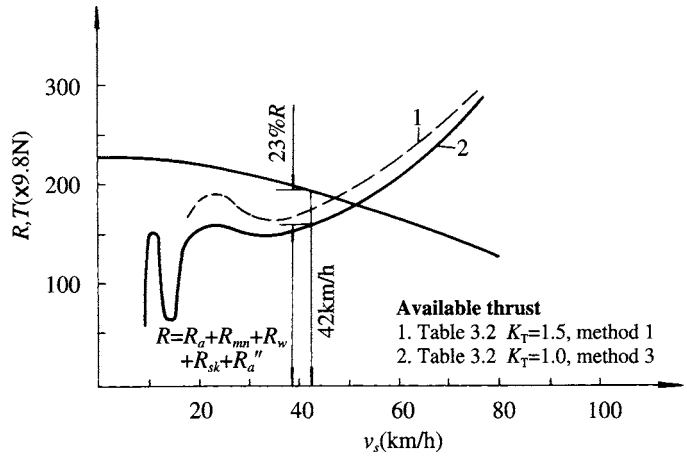

Fig. 3.31 Comparison of total drag of ACV model 7202 between calculations and measurements. $w = 2.775$t, $l_1/B_c = 2.14$, $p_c/l_c = 11.96$, $C_a = 0.6$, $\alpha'' = 0.5°$

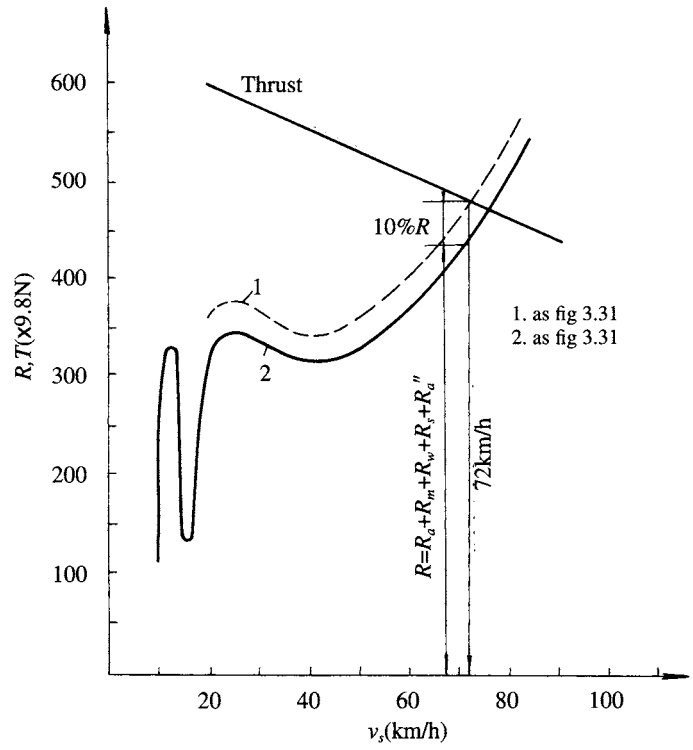

Fig. 3.32 Comparison of total drag of ACV model 711-IIA between calculations and measurements. $w = 6.4$t, $l_1/B_c = 2.15$, $p_c/l_c = 12{,}54$, $C_a = 0.4$, $\alpha'' = 0.25°$

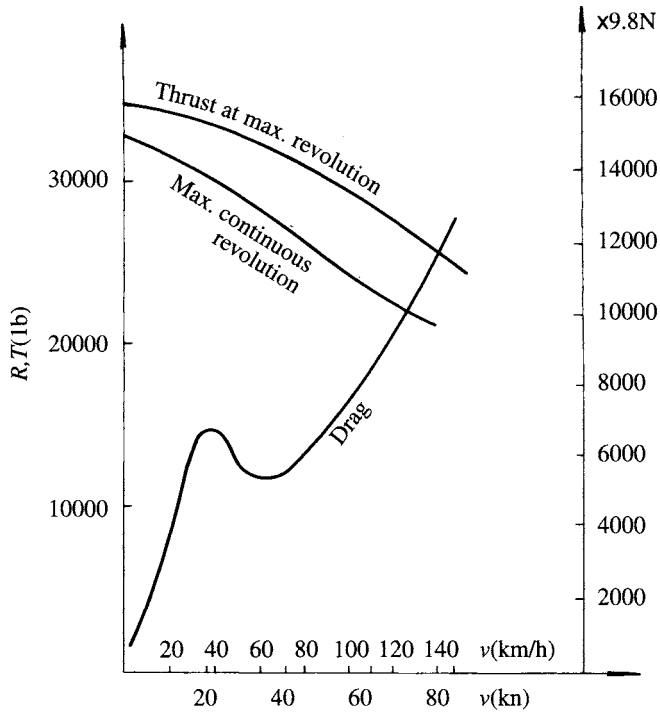

Fig. 3.33 The drag and thrust curves of SR.N4.

etc.) is included in the air profile drag, because in general the air profile drag coefficient C_a, which can be obtained either by model experimental data or by the data from prototype craft or statistical data, implicitly includes appendage drag in the coefficient.

- Similarly to conventional ships, model drag can be converted to drag of full scale craft according to the Froude scaling laws (see Chapter 9).
- Taking the Chinese ACV model 7202 and 711-IIA as examples, we calculate the drag components for these craft as shown in Figs 3.31 and 3.32. The propeller thrust in the figure was calculated according to the standard method for predicting the air propeller performance published by the British Royal Aeronautical Society. If K_T is assumed equal to 1.23 and 1.1 for craft 7202 and 711-IIA respectively and method 3 is used, then the calculated results agree well with the trial result.

  When MARIC used method No. 1, taking K_T as 1.65 for craft 7202 and 1.5 for craft 711-IIA, then the calculations agreed with test results. It can be seen that method 1 is approximate, because of the large K_T value.
- A typical resistance curve for the British SR.N4 can be seen in Fig. 3.33.

SES

There are many methods for calculating the drag components of an SES as are mentioned above, though one has to use these methods carefully and not mix them with

Table 3.3 Methods for calculating the drag of SES over calm water

Method	Method 1 Estimation	Method 2 Conversion from model tests	Method 3 NPL Method	Method 4	Method 5 Kolezaev Method
Drag items					
Aerodynamic profile drag			$R_a = 0.5\rho\ C_a\ S_a\ v^2$		
Wave-making drag due to air cushion			$R_m = \rho_a\ Q\ v$		
Friction drag of the sidewalls		$R_w = C_w\ p_c^2\ B_c/(\rho_w\ g)$ C_w can be obtained from Fig. 3.2 and 3.3			$R_w = C_w\ (4\ p_c\ W)/(\rho_w\ g\ l_c)$ C_w from Fig. 3.4
Wetted surface area of sidewalls			$R_{swf} = (C_f + \Delta C_f)\ S_f\ q_w$	$C_f = 0.455\ /\ [l\ g\ Re]^{2.58}$	$\Delta C_f = 0.0004$ approx
Residual drag of sidewalls	$R_w = 0.05\ C_w\ (p_c^2\ B_c)/(\rho_w\ g)$ where C_w is from Figs 3.2 and 3.3	R_{sww} is included in R_r		$R_{sww} = 0.05\ C_w\ (p_c^2\ B_c)/(\rho_w\ g)$ where C_w is from Figs 3.2 and 3.3	$R_{sww} = Kf_r\ W$ Kf_r from Fig. 3.30
Appendage drag		R_{ap} can be obtained by the same methods as for high-speed boats			Residual drag for sidewalls is included in appendage drag
Skirt drag or residual drag	$R_{sk} = k_s\ (R_w + R_a + R_m + R_{swf} + R_{sww} + R_{ap})$ or according to Fig. 3.19	$R_r = R_{tm} - (R_{wm} + R_{am} + R_{mm} + R_{swfm} + R_{apm})$ W/W_m		$R_{sk} = C_{sk}\ B_c\ h_c\ q_w$ C_{sk} from Fig. 3.17	$R_{sk} = (a + b\ Fr_d)\ B_c\ p_c\ v$ where $0.00225 \leqslant a \leqslant 0.021$, and $0.0015 \leqslant b \leqslant 0.0087$
Total drag	$R_T = R_w + R_a + R_m + R_{swf} + R_{sk} + R_{sww} + R_{ap} + R_{mw}$	$R_T = R_w + R_a + R_m + R_{swf} + R_{ap} + R_r$		$R_T = R_w + R_a + R_m + R_{swf} + R_{sk} + R_{ap} + R_{sww}$	$R_T = R_w + R_a + R_m + R_{swf} + R_{sk} + R_{sww}$
Remarks				If the craft is at optimum trim angle then use C_{sk} as shown in Fig. 3.17, otherwise increment.	

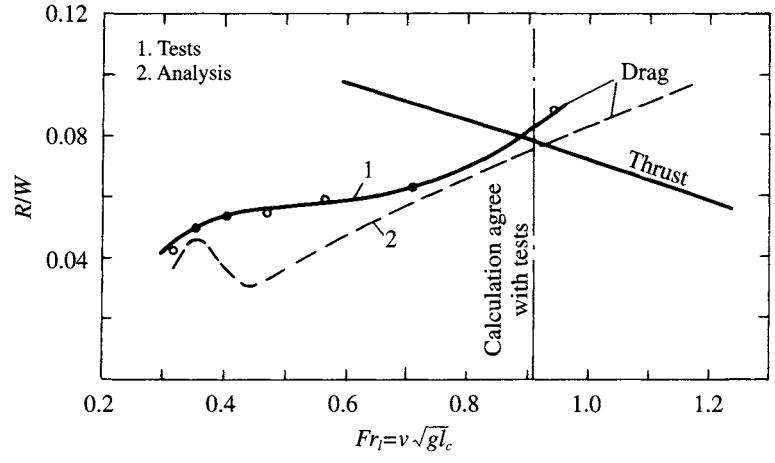

Fig. 3.34 The drag and thrust curves of 717C.

each other, otherwise errors may be made. We introduce five methods for SES total drag reference, outlined in Table 3.3 and add some commentary as follows:

1. It is suggested that method 1 can be used at the preliminary design stage and by comparison with methods 3, 4 and 5. With respect to method 2, this can be used at the final period of preliminary design or the detailed design stage.
2. The key problems for predicting the friction resistance of sidewalls are to determine accurately the wetted surface area. Of course it can be obtained by model tests in a towing tank. However, it can also be estimated by Figs 3.24, 3.25 and 3.27.
3. The sidewall residual drag (or sidewall wave-making drag) can be calculated according to Table 3.3, i.e. one can use the Newman method to calculate the wave-making drag (use Fig. 3.2 and 3.3) due to the air cushion, then take 5% of this as the sidewall residual drag. In the case of small buoyancy provided by the sidewalls ($W_s/W < 0.2$) the total wave-making drag can be calculated by the equivalent cushion method. The sidewall resistance can also be estimated by equation (3.43) or the Kolezaev method.
4. Seal drag R_{sk} can be calculated by the statistical method (MARIC method) or by taking 25–40% of total resistance (except R_{sk} itself) as the seal drag.
5. Taking Chinese SES model 717 as an example measurements and calculations are as shown in Fig. 3.34. It is found that the calculation results agree quite well with the test results, The typical SES resistance curve can be seen in Fig. 3.1.

3.13 ACV skirt/terrain interaction drag

For an ACV which operates mainly over land, such as self-propelled air cushion platforms, it is important to accurately determine the skirt/terrain interaction drag, as it

is a high percentage of the total drag. The total overland drag of ACV can be written as follows:

$$R_{gacv} = R_a + R_m + R_{sp} + R_{si} + R_{sk} \tag{3.50}$$

where R_{gacv} is the total overland drag of ACV (N), R_a the aerodynamic profile drag (N), R_m the aerodynamic momentum drag (N), R_{sp} the spray (debris) momentum drag (N), R_{si} the slope drag (N) and R_{sk} the skirt/terrain interaction drag (N).

R_a, R_m can be calculated by the methods outlined above. R_{sp} can usually be neglected due to the craft's low speed. The slope drag can be calculated according to the geography of the terrain. The skirt/terrain interaction drag is very strongly sensitive to lift air flow and is a function of craft speed and terrain condition. It is difficult to determine analytically and is usually determined from experimental data.

The overland drag curve of an ACV can be divided in three modes controlled by cushion flow rate as shown in Fig. 3.35:

1. Mode A, ACV profiles the terrain perfectly (i.e. a clear air gap between ACV and terrain);
2. Mode B, ACV experiences strong skirt/terrain interaction effects;
3. Mode C, ACV operates in 'ski' mode.

In mode A, at high flow rates, drag is relatively low. Normally in this flow region there is an air gap under most of the skirt periphery. In mode B, segment tips drag on the surface, but the delta regions between skirt tips still exist. In mode C, segment tips are pressed against the surface and the air flow acts more as a lubricant.

Figure 3.35 shows that the skirt/terrain interaction drag is closely related to skirt tip air gap. According to Chapter 2, the lift air flow Q can be written as

$$Q = l_j\, h\, \phi\, [2p_c/\rho_a]^{0.5} \tag{3.51}$$

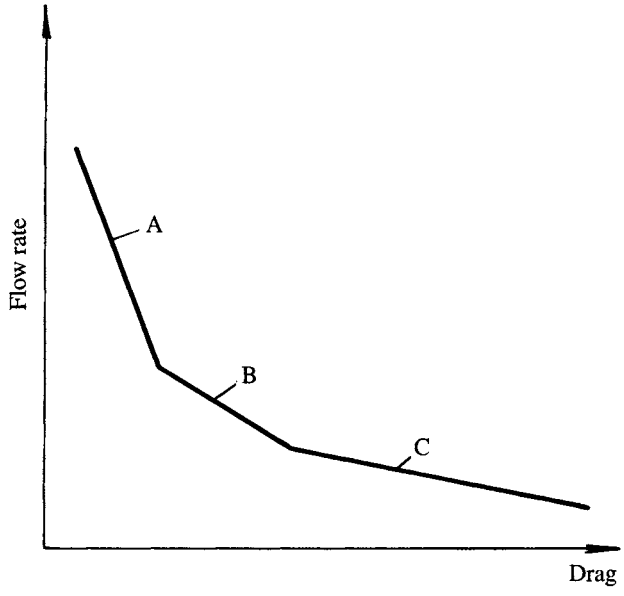

Fig. 3.35 Three operation modes of an ACV over ground terrain.

where Q is the lift air flow (m^3), l_j the peripheral length of the skirts (m), h the skirt clearance, including the equivalent clearance regarding the air leakage from the delta area of fingers, ϕ the air flow discharge coefficient and p_c the cushion pressure (N/m^2).

Different terrain conditions can radically change the effective discharge coefficient, (see Table 3.5). Grass or rock have the greatest effect. It is inappropriate therefore to characterize the air gap by h alone, since rough terrain and stiff grasses or reeds will reduce the skirt clearance significantly at the same air flow.

Fowler [36] defined $h_f K$ as the gap height instead of using h alone (i.e. $h_f K = h$), where K is referred directly to the terrain condition. This gap height for various craft is shown in Table 3.4. Then it can be seen that a high gap height $h_f K$ is normal for a high-speed ACV and low $h_f K$ for hover platforms.

Test results demonstrating the relation between skirt/terrain interaction drag and $h_f K$ as well as the terrain conditions are shown in Fig. 3.36 [36]. It is clear that the skirt/terrain interaction drag is very strongly sensitive to lift air flow.

Skirt/terrain interaction drag will increase at a higher rate as the skirt air gap is reduced below a critical value. For this reason, an optimum skirt air gap has to be selected as shown in Table 3.5 [37], recommended by Fowler.

Figure 3.37 shows the relation between the skirt/terrain interaction drag and craft speed. Figure 3.38 shows the drag for craft running on an ice surface in relation to the Froude number. These test results are provided for reference.

Table 3.4 Gap height $h_f K$ of various ACV

Item	Craft	Type	$h_f K$
1	SR.N5	ACV	0.08
2	SR.N6	ACV	0.07
3	SR.N4	ACV	0.084
4	SR.N4 Mk2	ACV	0.073
5	*Voyageur*	ACV	0.08
6	*Viking*	ACV	0.068
7	LACV–30	ACV	0.062
8	ACT 100	ACP	0.019
9	*Sea Pearl*	ACP	0.018
10	*Yukon Princess*	ACP	0.012
11	Hex–55	ACP	0.018
12	Hex–1B	ACP	0.015

Table 3.5 The suggested gap height $h_f K$ for various ACV terrain conditions [36]

Ground terrain	$h_f K$	K	Drag coefficient %
Smooth concrete, slow speed	0.0035	1.0	2
Firm snow	0.0055	1.5	2.5
Short grass	0.02	6	2
Moderate grass	0.02	6	2
Long reedy grass (1st pass)	0.022	6	40
Long reedy grass (10th pass)	0.022	6	5
Crushed rock	0.02	6	15–30
Mudflats	0.016	5	2–5
Concrete, high speed	0.013	4	2

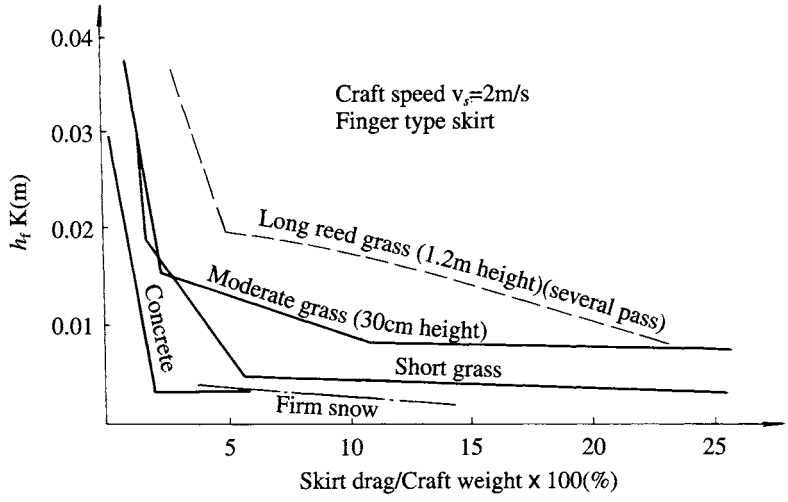

Fig. 3.36 Skirt ground interference drag as a function of surface condition and ACV equivalent air gap h_f K. [37]

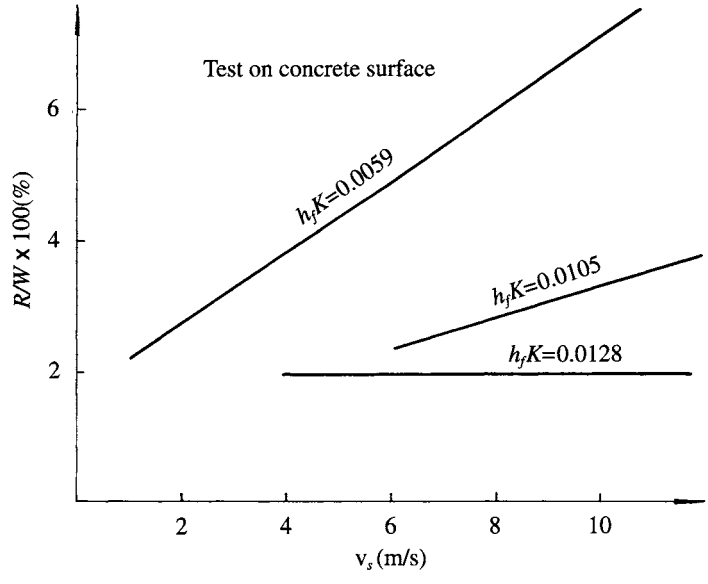

Fig. 3.37 Skirt ground interference drag as a function of $h_f K$ and craft speed.

3.14 Problems concerning ACV/SES take-off

The acceleration capability of ACV/SES through hump speed is a very important design feature. Designers and users are therefore often concerned about the 'take-off' capabilities of ACV/SES running over water, because the hump speed is only one-

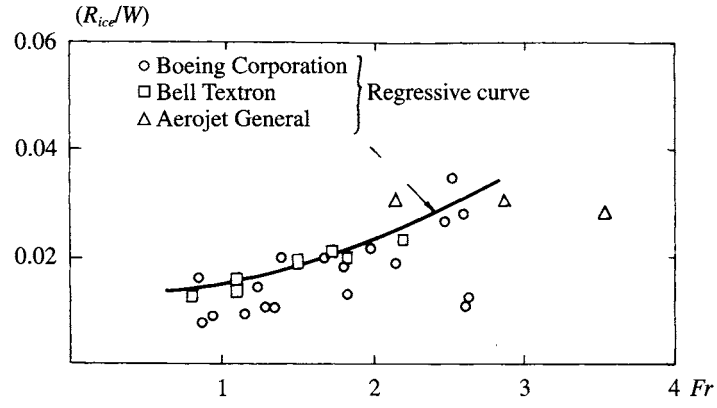

Fig. 3.38 Skirt drag of ACV running on ice as a function of *Fr*.

third to one-fifth of normal design speed. The physical phenomenon of take-off is therefore considered here and some comments on craft optimization presented.

When craft speed increases, at *Fr* of about 0.38 the craft begins to ride between two wave peaks located at the bow and stern respectively. The midship portion of the craft is then located at a wave hollow and a large outflow of cushion air blowing up water spray is clearly observed in this region, as shown in Figs 3.18(c) and 3.39. This in turn reduces the air gap below the bow and stern, which in the present case with wave peaks located at the bow and stern seals, would result in contact of water with the planing surface of the seals and present a new source of drag acting on the craft.

This condition was investigated by MARIC by towing tank model experiments. The surface profile was obtained with aid of a periscope and photography [28].

Seal drag consists of two parts. One part is the induced wave drag of the seals and the other is frictional drag acting on the planing surfaces. A large amount of induced wave drag can be built up when the seals are deeply immersed in water and the planing surfaces contact at large angles of attack.

The skirt-induced wave is also superimposed on the wave system induced by internal cushion pressure and constitutes secondary drag. In the case of poorly designed seals or skirts, the peak drag at $Fr = 0.38$ may be larger than that at $Fr = 0.56$ (main resistance hump speed). Meanwhile, transverse stability will most probably also decrease.

A craft will tend to pitch bow down when the craft has a rigid stern seal (such as fixed planing plate with a large angle of attack or a balanced rigid stern seal) and a relatively flexible bow seal. The craft will most probably be running at a large yawing angle as well, due to poor course stability. The operator of the ACV or SES will be obliged to use the rudder more frequently.

The forces arising from these situations are complicated and quite large in magnitude. Meanwhile the ship may be difficult to control, the propulsion engines are overloaded and a lot of water spray is blown off from the air cushion and flies around the craft, interfering with the driver's vision, making handling of the craft even more difficult. Operation would probably become very complicated if the sea were rough rather than the calm conditions considered in this chapter. Such phenomena are the features of a craft failing to accelerate successfully through secondary hump speed.

Meanwhile, if the thrust of the propellers is larger than the resistance of the craft,

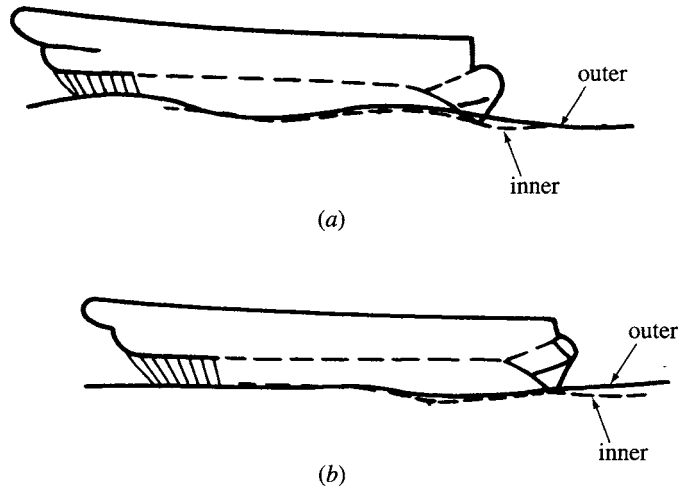

Fig. 3.39 Inner/outer water lines of an SES model at $Fr_l = 0.38$(a), $Fr_l = 0.51$(b).

then the craft speed will increase so as to move to the wave trough position. The main resistance hump occurs at $Fr = 0.56$. In this case the craft is located on the wave with the wave peak at the bow and the trough at the stern (wavelength is twice craft length) and the craft has maximum trim angle. The craft drag will generally drop down once the speed of the craft is over the secondary hump speed (i.e. $Fr = 0.38$) and the craft will accelerate to run over the main hump speed ($Fr = 0.56$) because the drag of the craft will be reduced due to the accelerating motion of the craft.

On an SES, the main propulsion engines normally cannot provide full thrust, due to the lower speed of advance at the secondary hump ($Fr = 0.38$). Smooth transition through hump speed then depends on the margin of thrust included by the designer at secondary hump speed, which will be the source of accelerating thrust. If this is too low, then transition will be very slow, as was the case with early SESs.

When the craft accelerates continuously, the wave trough will then move to the stern and the craft will be accelerated, so long as the skirt elements do not scoop; meanwhile the craft should travel with good course stability, transverse stability, little spray and beautiful running attitude to give the crew or passengers an excellent feeling (Fig. 3.18(b)). For this reason, the running attitude is rather different for the pre- and post-hump speed. Whether or not the craft can pass though the hump speed depends on such factors as the characteristics of the seals/skirts, the cushion pressure length ratio, the transverse stability of the craft and the correct handling of the craft.

In the early days of hovercraft research, people used to worry about whether the hovercraft could ever ride over the hump speed. It seemed merely to be a stroke of luck, because of poorly designed seal/skirt configurations or using rigid bow/stern seals which lead to a large additional wave-making drag.

From the point of view of craft drag (other factors will be discussed later), the factors influencing take-off can be summarized as follows:

- magnitude of resistance peak, especially at secondary hump speed ($Fr = 0.38$);

- the added wave-making drag due to seal/skirt at secondary hump speed and the flexibility of skirts to yield to waves without scooping;
- the ability of the craft to keep straight course stability and good transverse stability during take-off through hump speed.

It is not difficult to improve the ability to accelerate through hump speed if the factors mentioned above are taken into account. According to research experience at MARIC, we give some examples to illustrate these factors for the reader's reference.

1. The ACV model 711, the first Chinese amphibious test hovercraft, was found to suffer difficulties on passing through hump speed in 1965. The craft, weighing 4 t, was powered by propulsion engines rated 191 kW and obtained a thrust of 5000 N during take-off. This meant that the thrust/lift ratio of the craft was about 1/8. It was difficult to get the craft to take off, owing to large water-scooping drag of the peripheral jetted nozzle and shorter extended flexible nozzle, especially at the stern position. After a time, MARIC used the controlling valve of the air duct to adjust the running attitude of the craft in order to decrease the water contact drag of the skirt and the craft successfully passed though the hump speed.
2. After a time, craft model 711 had been chosen to mount a flexible skirt. The take-off ability of the craft was improved significantly due to the enlarged air cushion area, which reduced the cushion pressure and cushion pressure–length ratio, and also the flexible skirts' ability to yield to the wave hump. The wave-making drag at secondary hump speed was reduced by the same modifications.
3. The modified craft model 711 with flexible skirts was occasionally found to suffer difficulties in passing though the hump speed. The flexible jetted bag stern skirt with relatively larger area forward (Fig. 3.40) induced large skirt drag during take-off because the stern skirt took a form allowing scooping. It was observed that sometimes the original craft could still struggle to cross over the hump speed after a long running time. A breakthough occurred (literally!) after the diaphragms of the jetted skirt were accidentally broken and the stern skirt had changed from A to B as shown in Fig. 3.40.
4. The probability of successful take-off for the first Chinese experimental SES, the 711 in 1967, was about 60–70%, and it could be improved by retracting the stern seal during the course of passing though the hump speed (Fig. 3.41) and reached 100% take-off probability. This was a successful method for the following reasons:

   (a) Drag due to water scooping was reduced by decreasing the water scooping area of the stern seal as the stern seal is raised.
   (b) Angle of attack of the stern seal was reduced with consequential reduction in drag.
   (c) The running attitude was changed to a trimmed condition with bow up; as a result the bow seal drag was reduced and the course stability was also enhanced.

   It was noted that similar methods have been developed in other countries. For instance, there was a retractable stern seal mounted on the Soviet passenger craft *Gorkovchanin* and similar equipment was also mounted on the US test craft XR-3 to improve the dynamic stability during take-off, as shown in Fig. 3.42. Figure 3.42 shows that hump drag can be reduced considerably by retracting the stern seal.
5. When the Jin-Sah river passenger SES with the balanced rigid seal performed

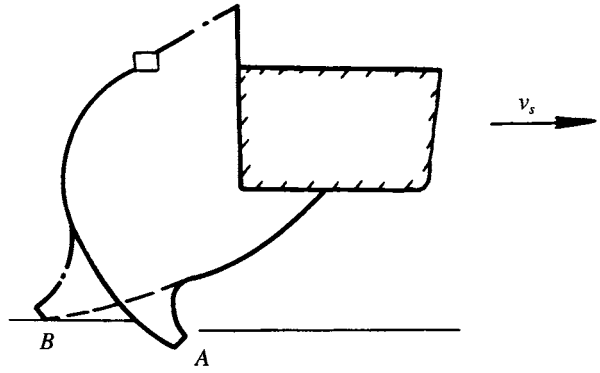

Fig. 3.40 Sketch of skirts with bag and jetted extensions.

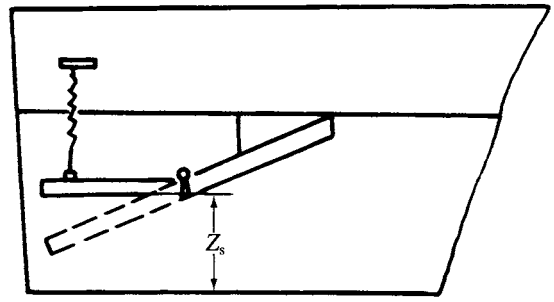

Fig. 3.41 Rigid stern seal with the function of controlling the air gap.

trials on water in 1970, it was found that a large amount of drag also acted on the stern, and as a result it was difficult for the craft to pass through hump speed. This may be traced to the following reasons:

(a) Suppose the stern seal was balanced hydrodynamically so that the lift moment (about point B in Fig. 3.43) due to the rear part of the seal would be greater than that due to the fore part of the seal. The stern seal plate would assume a negative angle of attack with the flexible nylon cloth taking the form of a concave bucket as shown by line 2 in Fig. 3.43. This would lead to a large amount of stern seal drag and it would be difficult for the craft to take off.

(b) On the other hand, if the hinge of the stern seal were moved to the rear with a longer nylon cloth, then it would take up the form of line 2 in Fig. 3.43. Here although the lift moment of the fore part would be greater than that of the rear part, forming a positive angle of attack, the planing surface is discontinuous, which would lead to a large amount of drag. In such a case the drag of the stern seal would be so large that it would be impossible to take off. The normal form of the stern seal is as shown in line 1 of Fig. 3.43 with proper length of nylon cloth to combine with the proper position of the hinge. In this case it is easy for the craft to take off.

6. The SES version 719 with bag and finger type skirt for bow seal and twin bag for

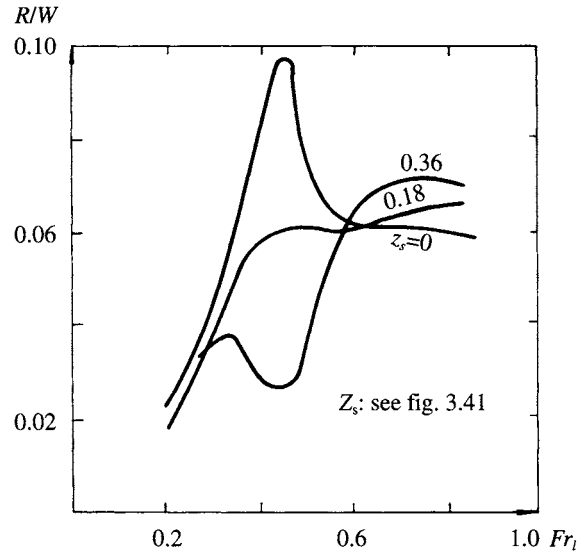

Fig. 3.42 Influence of the vertical distance between the base-line and lower tip of stern seal Z_s on drag ratio *R/W*.

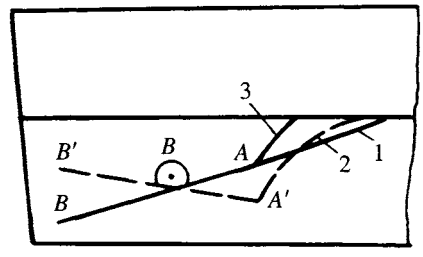

Fig. 3.43 Various locations of balanced type stern seal. 1, 2, 3: flexible connection seal; AB, A'B': two modes for solid seal.

stern seal took off very easily because of good yielding features of the skirts in waves. After a time, the craft was extended by 6 m and L_c/B_c stretched from 4 to 5.05 and reduced cushion pressure–length ratio from 17.6 to 14.6 kgf/m. For this reason, the peak wave-making drag was reduced drastically and moved the hump speed to larger *Fr*. Therefore, the engines could supply more power because of the large magnitude of the hump speed. Take-off performance improved greatly, with shortened time for take-off and less spray.

3.15 Effect of various factors on drag

The themes to be discussed here are the problems related to the drag of craft running over calm water. The performance on rough sea will be discussed in Chapter 8. Since the hovercraft, especially ACVs, travels close to the water surface at high speed, the drag will increase dramatically as soon as the skirts come into contact with the water surface occasionally making the drag unstable in magnitude. The effect of various factors on the craft performance are as follows.

The effect of position of LCG

The effect of LCG on craft drag, mainly skirt drag, is deterministic. A slight change of LCG will lead directly to varying craft drag due to its effect on bow and stern skirt friction, especially in the case of poorly designed bow/stern skirts.

With respect to SES, especially SES with thin sidewalls, the change of LCG will also lead to a draft change at bow/stern seals, increasing seal drag, in the case of no transverse cushion compartmentation on an SES. Figure 3.44 shows the effect of LCG on drag of an SES based on model testing data. It can be seen that when the centre of gravity of the model is moved just 3% of L_c, a drag increase of about 70% may result. Figure 3.45 [30] shows the relation between lift–drag ratio and trim angle of the US SES-100B. It is clear that the deviation of trim angle from an optimum of about 2° leads to an increase in drag about twice at a speed of 40 knots.

Figure 3.46 shows the influence of LCG on the speed of SES model 717C during trials. For this reason, it is necessary to determine the LCG carefully. Based on

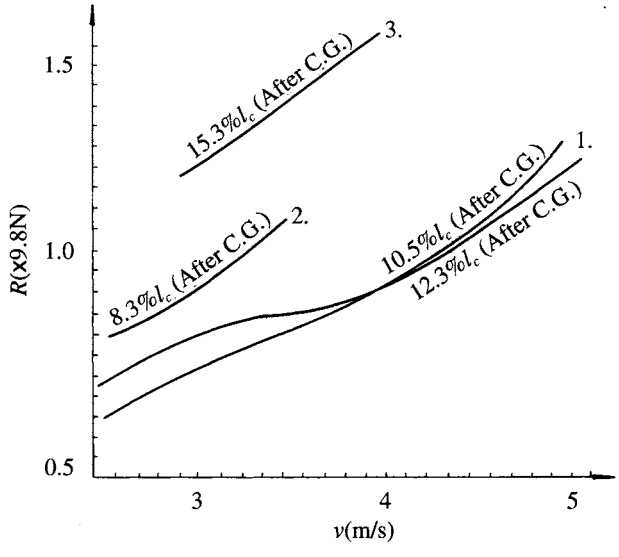

Fig. 3.44 Influence of longitudinal centre of gravity on total drag of SES model. 1: $P_c/l_c = 15.4$, 2: $P_c/l_c = 17.3$, 3: $P_c/l_c = 19.4$.

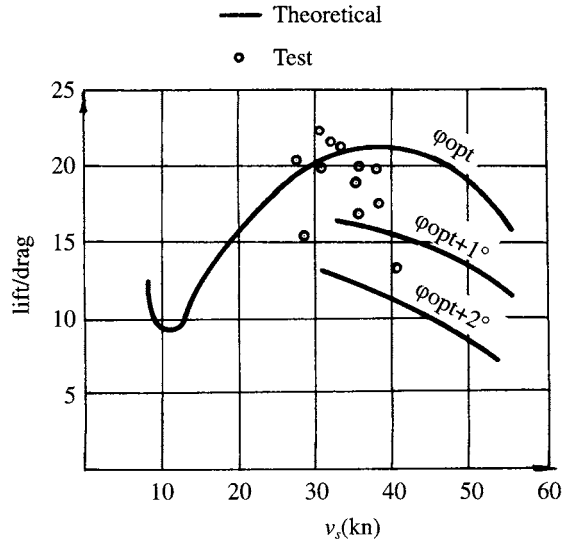

Fig. 3.45 Lift-weight ratio of SES-100B vs trim angles and craft speed.

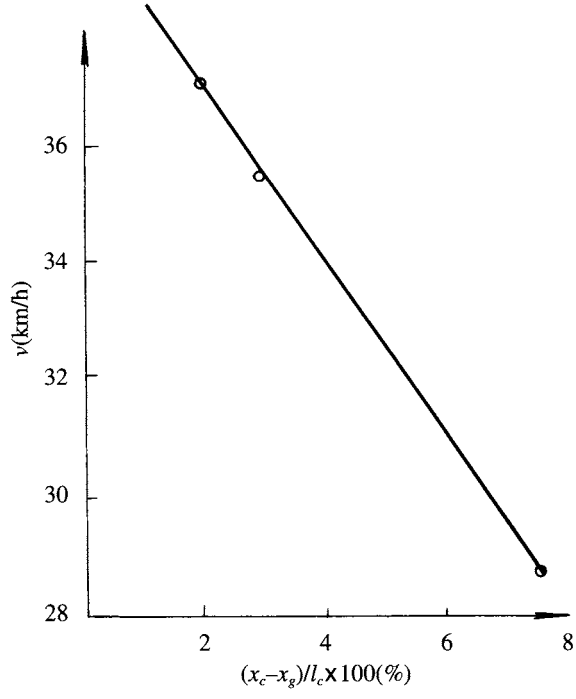

Fig. 3.46 Influence of longitudinal centre of gravity on speed of craft model 717C.

MARIC experience and ref. 39, it is suggested that the LCG of an SES (also an ACV) should normally be in the range

$$(X_g - X_c)/L_c \approx -(0 \sim 0.5)\% \text{ [aft of CG.]}$$

where X_g is the LCG, measured from the stern, X_c the longitudinal centre of buoyancy, measured from the stern and L_c the cushion length.

Effect of cushion pressure–length ratio

Wave-making drag increases in proportion to the square of cushion pressure. Cushion pressure also affects the craft outer draft, therefore the cushion pressure seriously affects the craft drag. The effect of cushion pressure on hump drag will be further increased in the case of poorly designed skirt/seals. Figure 3.47 shows the effect of cushion pressure of an SES model on drag, while Fig. 3.48 shows the effect of various cushion pressure / length ratios on the drag of craft tested in a towing tank at different times.

Effect of inner draft (t_i)

Hump drag will decrease in the case of increasing the inner draft of an SES during take-off, because air leakage from the cushion is decreased amidships, decreasing the cushion pushing/scooping drag of the bow/stern seals. The drag of SES will also increase at the post hump speed in the case of increasing the inner draft, because this will lead to an enlarged wetted surface of the sidewalls. Figure 3.49 shows the effect of inner draft change on drag of an SES model running on calm water.

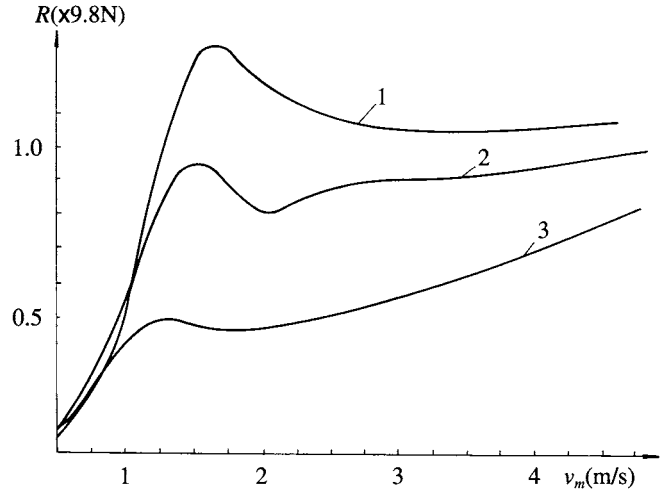

Fig. 3.47 Influence of cushion length/beam ratio and p_c/l_c on total drag of craft models. 1, 2, 3: see Fig. 3.44.

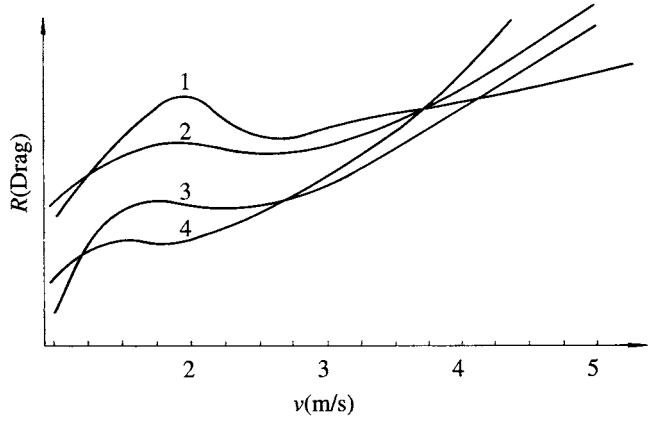

Fig. 3.48 Influence of cushion length/beam ratio on total drag of craft models in different test tanks. 1: tests in MARIC $p_c/l_c = 20$; 2: same model, thicker skirt, different tank; 3: as 2, $p_c/l_c = 15.7$; 4: as 3, but in MARIC tank.

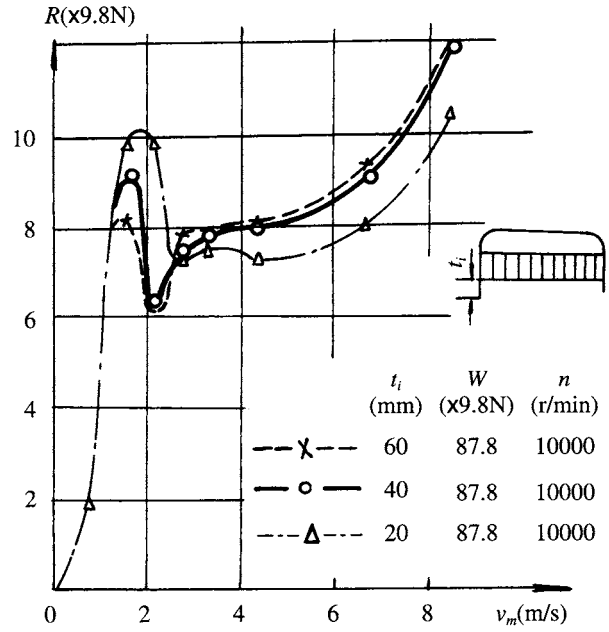

Fig. 3.49 Influence of inner draft of sidewalls t_i on total drag of SES model on still water.

Effect of air flow rate

It is probable that the air flow coefficient $\bar{Q}$ magnitude will not affect the take-off performance of hovercraft (except too small values of $\bar{Q}$) when the skirt has been carefully designed, because of the good wave-yielding performance for flexible skirts. However, craft drag at post-hump speeds will be closely related to $\bar{Q}$. Therefore, the

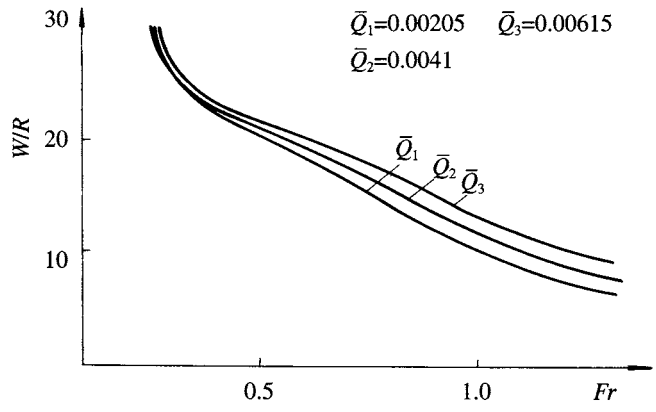

Fig. 3.50 Influence of cushion air flow rate on Lift/drag ratio of SES on calm water.

importance of air flow rate of a modern ACV/SES is rather more significant than early ACV/SES craft, which were generally designed with high cushion flow rates. In the latter case, a large gap height was pursued in order to reduce the contact drag of the bow/stern skirt, but in the former, it seems unnecessary to design a large gap height due to the beneficial properties of the flexible skirt.

The air flow still affects spray drag and water friction drag at post-hump speeds, because a large air flow rate will increase the air component of the two-phase flow blown from the air cushion, producing air lubrication effects on the stern skirt/seal. This can be clearly seen in Fig. 3.50.

In the case where the $\bar{Q}$ is so small as to cause significant immersion of skirts, the take-off performance will deteriorate. For example, a Chinese ACV with too small air flow could run over the hump speed on calm water, but could not take off even in small head winds and waves. Take-off performance was improved by increasing the lift power by 15%.

Effect of skirt configuration

The configurations of skirts are strongly sensitive to the craft drag. Figure 3.51 shows the effect of both rigid and flexible seals on drag of an SES. It can be clearly seen that the drag of craft with a flexible skirt is less than that with a rigid seal by a significant margin. Table 3.6 demonstrates that the drag coefficient for skirts of French ACVs improved significantly over eight years.

Table 3.6 The improvement of skirt drag coefficient of French ACVs over several years

Time interval	Craft model	Skirt drag coefficient
June 1968–June 1969	N102	0.36–0.42
Sept. 1967–March 1969	N300-02A	0.16–0.22
March 1969–June 1970	N102C	0.26–0.32
July 1970–June 1971	N102L	0.26–0.32
June 1973–Feb 1975	N300–02B	0.05–0.12
1973–1976	N500 (model)	0.05–0.07

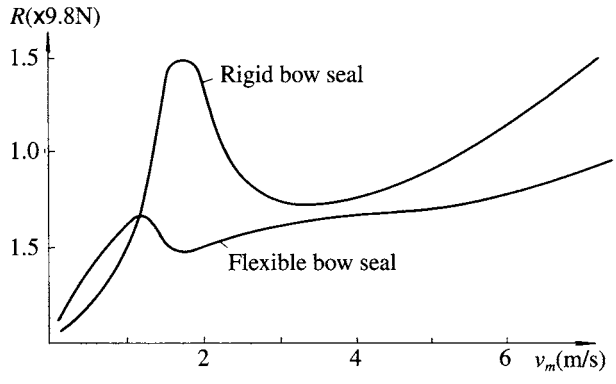

Fig. 3.51 Influence of seal types on total drag of SES: (a) with rigid bow seal; (b) with flexible bow seal.

Summary

Many factors affect craft drag. Due to the drag peak between displacement and planing mode of operation, this has been one of the challenges for designers, manufacturers and operators to try to minimize.

Efficient skirt systems can greatly improve drag and therefore attention has to be paid to optimizing this system if an ACV or SES is to be a successful design. Skirts are discussed in detail in Chapters 7 (theory) and 13 (design). As an example, by adopting the fixed planing stern seal for SES model 717, this obtained a stable cruising speed of 43 km/h, while adopting the balanced planing stern seal, the drag of the craft was very unstable and at full power the craft speed fluctuated between 57 and 50 km/h. From our point of view a craft with a stable speed of 55 km/h is better than one with an unstable speed sometimes at 60 km/h and sometimes at 50 km/h!